

ESTIMATION OF EVAPOTRANSPIRATION USING ADVECTION ARIDITY APPROACH

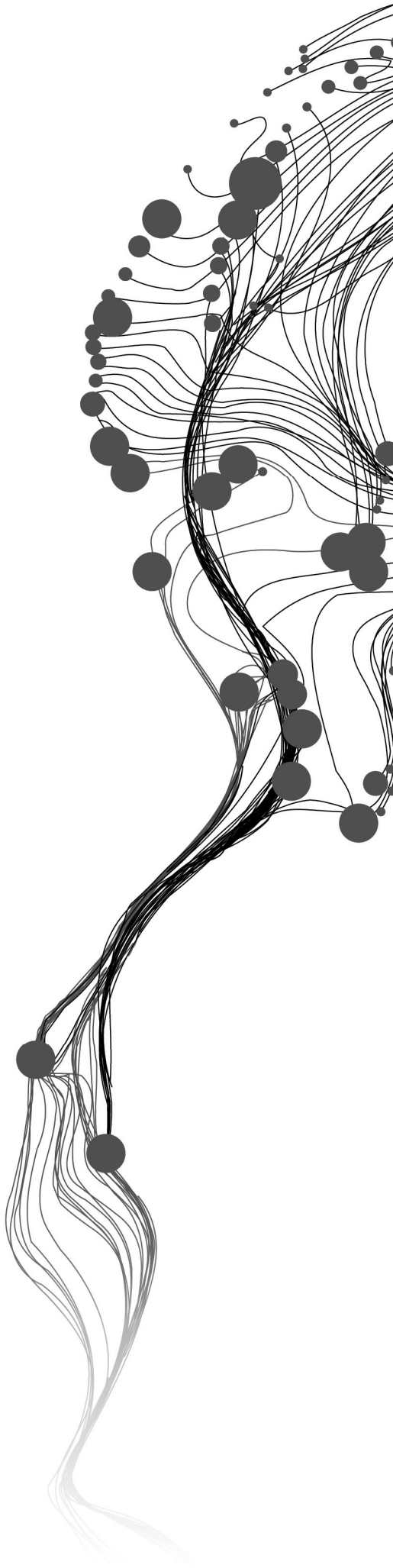
YESRIB BAHIRU SHIFA]

Enschede, The Netherlands, [March, 2011]

SUPERVISORS:

Dr.Ir., C., van der Tol

Ir., J, Timmermans



ESTIMATION OF EVAPOTRANSPIRATION USING ADVECTION ARIDITY APPROACH

YESRIB BAHIRU SHIFA]

Enschede, The Netherlands, [March, 2011]

Thesis submitted to the Faculty of Geo-Information Science and Earth Observation of the University of Twente in partial fulfilment of the requirements for the degree of Master of Science in Geo-information Science and Earth Observation.

Specialization: Water resource and environmental management

SUPERVISORS:

Dr.Ir., C., van der Tol

Ir., J, Timmermans

THESIS ASSESSMENT BOARD:

Prof.Dr., Z., Su(Chair]

Dr., R., Roebeling (External Examiner, KNMI)

DISCLAIMER

This document describes work undertaken as part of a programme of study at the Faculty of Geo-Information Science and Earth Observation of the University of Twente. All views and opinions expressed therein remain the sole responsibility of the author, and do not necessarily represent those of the Faculty.

ABSTRACT

The AA model was tested with both daily and half hourly data for the relatively wet and dry condition in Sardon, Spain. The wind function which was applied to the AA model was standard, measured and empirically calibrated. Those three wind function validated by both measured eddy tower evapotranspiration and complementary relationships, which is the bases for AA model. The daily result shows that for relatively wet conditions of integrated wind function of standard, measured and calibrated into advection aridity (AA) model is in a good agreement with actual evapotranspiration (ET). However for dry the only was calibrated AA model, but less efficient compared to wet condition of those three wind function. The statistics of standard and measured AA model in dry condition shows that the RMSE (root mean square error) were 0.95 mm/day and 1.5 mm/day, respectively. Under dry condition, both standard and measured AA model overestimated. By mid of the May to mid of June, the standard estimates 46% higher than the eddy tower measured ET. The measured wind function estimates two times higher than the actual eddy tower ET. The calibrated AA model in dry condition was better than the preceding overestimated standard and measured wind functions. The RMSE was 0.68 mm/day and the trend was evaluated in a good agreement with the complementary relationship. For the higher temporal resolution, the half hourly AA model increases the discrepancy and shows no clear complementary relationship trend between the standardized actual ET and Potential ET.

ACKNOWLEDGEMENTS

This research would have not been a lot less easy without the help and support of many people. It is a great pleasure for me to acknowledge those who contribute to the success of my M.Sc. thesis studying.

First, I would like to thanks my first supervisor, Dr. Ir. C van der Tol for his excellent guidance and encouragement throughout my study period. I highly appreciate his constructive criticism and valuable advise which helped me to improve a lot and the way how he threat his students influenced me to have strong patient to finish my research. I hope our relation will continue in the future. Keep it up!! Thank you so much!!

My acknowledgement with high appreciation goes to second supervisor Ir. J. Timmermans for guiding me with valuable comment and editing my research and his famous saying "...oh... this is easy on Matlab...helped me a lot to improve my research skills.

I would like to thanks my field work staffs: Leonardo Reyes, Enrico Balugani, Alain Frances, Gabriel Parodi and my colleague having good time passed away.

Thanks to the water Resource Department of ITC, my classmates and all Ethiopian community in Enschede for the wonderful time we have together.

My acknowledgement goes to the Netherlands organization for international cooperation in higher education that funded my study.

Especial thanks goes to my Brother Abdulaziz who helped me a lot during the stay in Netherlands and all my beloved family support and prayers.

TABLE OF CONTENTS

Abstract.....	i
Acknowledgements	ii
1. introduction	1
1.1. Background and Relevance.....	1
1.2. General Objective.....	2
1.3. Research Questions.....	2
1.4. Research Output.....	2
1.5. Structure of the Thesis	2
2. theoretical background.....	3
2.1. Introduction	3
2.2. Complementary Relationships	4
2.3. Potential Evapotranspiration(Penman model).....	5
2.4. Aridity Advection Model and Proposed Formulations	6
2.5. Wind Function and AA model.....	6
2.6. Normalized Evapotranspiration	8
3. study area.....	11
3.1. The Data and Measuring Instrument.....	12
4. methods	15
4.1. Methodology frame work.....	16
4.2. Data Set.....	17
4.3. Meteorological Parameter	18
4.4. Net radiation.....	21
4.5. Energy Balance	22
4.6. Evapotranspiration.....	24
5. Results and discussion.....	25
5.1. Comparison of Priestley – Taylor(PT) Model and Measured Evapotranspiration.....	25
5.2. AA Model Validation for Standard Wind Function.....	26
5.3. AA Model Validation for Measured Wind Function	28
5.4. AA Model Validation for Calibrated Wind Function	31
5.5. Half hourly AA Model Validation.....	33
6. conclusions and outlook.....	37
6.1. Conclusions	37
6.2. Outlook	38

LIST OF FIGURES

Figure 2-1 : Sketch illustrates the complementary relationship between the ET_a and ET_p for varying moisture condition in terms of moisture index, ET_a/ET_{po}	9
Figure 3-1 : Map of the Study area.....	11
Figure 3-2 : Daily mean air temperature from 120-210 Julian days in 2010	12
Figure 3-3 : a) To the left side is CSAT-3(Campbell Scientific, 1996) and CO ₂ /H ₂ O gas analyser LICOR L1 7500, b) to the right side includes all CSAT-3, CNR 1 Net Radiometer (Kipp & Zonen) and Vaisala in eddy tower Sardon, Spain.....	13
Figure 4-1 : Methodology flow chart.....	16
Figure 4-2 : Shows as temperature increases relative humidity decreases, inverse relationship between temperature and relative humidity.	20
Figure 4-3 : Shows slope of saturated vapour pressure (SSVP) of 30 minutes, and daily mean slope saturated vapour pressure (DMSSVP) is for the mean method and FAO 56 mean methods.....	21
Figure 4-4 : Net Radiation Budget for three days of dry season.....	22
Figure 4-5 : Surface energy balance flux for DOY 306 – 308.....	23
Figure 4-6: Energy balance closure: left side is half hourly and right side is daily energy balance closure. The x – axis is available energy ($R_n - G_o$ storage) and on the y – axis is the sum of sensible and latent heat flux.	23
Figure 5-1 : Comparison of average daily PT model with measured ET for the month March and April..	25
Figure 5-2 : AA model validation for standard wind function.....	28
Figure 5-3 : AA model validation for standard wind function under complementary relationship between normalized actual ET and normalized potential ET.....	28
Figure 5-4 : AA model validation for measured wind function.....	30
Figure 5-5 : AA model validation for measured wind function under complementary relationship between normalized actual ET and normalized potential ET.....	30
Figure 5-6 : AA model validation for a calibrated wind function.....	32
Figure 5-7 : AA model validation for daily calibrated wind function in terms of complementary relationship between actual ET and potential ET.....	32
Figure 5-8 : AA model validation for half hourly standard wind function	33
Figure 5-9 : AA model validation for half hourly standard wind function	34
Figure 5-10 : AA model validation for half hourly measured wind function.....	35
Figure 5-11 : AA model validation for half hourly measured wind function in terms of complementary relationship between actual and potential ET.....	35

LIST OF TABLES

Table 4-1 : Illustrates the three wind function integrated in the advection aridity model (AA model) and its product of model output.....	15
Table 4-2 : Pre-processed data. The parameter used in the model for both half hourly and daily	17
Table 4-3 : Processed product from the meteorological parameter and available energy	18
Table 4-4 : Some more properties of water vapour in Sardon.....	19
Table 4-5 : Illustrates a mean, minimum and maximum of radiation flux ($W m^{-2}$) in the study period 2010.....	22
Table 5-1: Rainfall, relative humidity and net radiation for some example days. The data show that net radiation is negatively correlated with rainfall and relative humidity.	26
Table 5-2 : shows the statistics of the results for all the daily analyses	26
Table 5-3 : Statistical result of daily measured AA ET in mm/day.....	29
Table 5-4 : Statistical result of half hourly measured AA and eddy tower measured ET in $W m^{-2}$	34

ABBREVIATION AND SYMBOLS

AA _s	Standard advection aridity model
AA _m	Measured advection aridity model
AA _c	Calibrated advection aridity model
ET	Evapotranspiration
ET _a	Actual evapotranspiration
ET _p	Potential evapotranspiration
ET _{po}	Wetted evapotranspiration
E _e	Equilibrium evapotranspiration
e_s	Saturated vapour pressure
e_a	Actual vapour pressure
Δ	Slope of saturated vapour pressure at air temperature
C _p	Specific heat of the air
$f(\bar{u})$	Wind function
u_*	Friction velocity
E_a	Drying power of the air
λ	Latent heat of vaporization
α	Priestley – Taylor coefficient
SW ↓	Short wave incoming radiation
LW ↑	Long wave outgoing radiation
H	Sensible heat flux
λET	Latent heat flux
k	Von Karman's constant
ρ	Density of the air
G_o	Ground heat flux
R_n	Net radiation
RMSE	Root mean square error

1. INTRODUCTION

1.1. Background and Relevance

In water limited environments, like Ethiopia, evapotranspiration plays the significant role in the hydrologic budget. Accurate evapotranspiration estimates are needed in a wide range of fields, like agriculture, hydrology, forestry and land management, and water resources planning, water balance computation, irrigation management, river flow forecasting, investigation of lake chemistry, ecosystem modelling (C. Y. Xu & Singh, 2005).

Accurate estimation of evapotranspiration helps for the African policy makers to prepare before drought comes and to forward the valuable information to agriculture sectors. In Ethiopia (2009), agriculture accounts for almost 41 percent of the GDP, 80 percent of exports, and 80 percent of the labour force. Many other economic activities also depend on agriculture, including marketing, processing, and export of agriculture products (http://en.wikipedia.org/wiki/Economy_of_Ethiopia). Estimating actual ET is of vital importance to Ethiopia. At present the National Meteorological Agency of Ethiopia uses the pan evaporation, which needs to be converted into actual evaporation using crop and environmental empirical coefficients. However actual evapotranspiration is difficult to measure, as it varies regionally and seasonally due to different climatic conditions, land uses, land covers, soil moisture content, and available radiation.

There are a lot of measuring techniques to estimate evapotranspiration. Both direct and indirect methods exist (e.g.WMO., 1994). Most measurement techniques require special instrumentation like eddy covariance, scintillometer, actinometer, pyranometer, and pyrgeometer etc. Such instrumentation is highly expensive, and consequently the majority of these measurement towers are found in western countries. In Ethiopia most stations do not carry all the specific instrumentation needed for detailed evapotranspiration measurements. The stations are either synoptic station, that only measures basic meteorological parameters, or World Meteorological Organization (WMO) stations (second and third class station), that only measure rainfall and temperature. It is therefore important for countries like Ethiopia to have a reliable evapotranspiration method that requires only a few meteorological parameters and can be routinely obtained at standard weather stations.

The Advection-Aridity model is one of the methods which require only meteorological parameter. This model was developed and validated by Brusaert (1979) during the drought of 1976. This validation was performed over a small rural catchment in the Netherlands with a time-step of three days, when at that the potential evapotranspiration far exceeded actual evapotranspiration. The model has so far not been tested well for other climate types. This research focuses on testing the model based for conditions, similar to the climate in Ethiopia, using eddy correlation ground observation data.

Though the advection aridity model proposed By Brutsaert (1979) for daily estimation, in this research both half hourly and daily was validated for relatively wet and dry condition. However no research has been performed to estimate and validate half hourly ET from the complementary relationship. Since Brutsaert (2005) mentioned that there is no a general accepted wind function, this needs to be investigated. There are several wind functions exist that can be integrated into the model. The wind functions are: (1) standard(Penman, 1948)(2) measured from friction velocity and wind speed(Thom,

1975; van der Tol et al., 2003) and (3) empirically calibrated (Morton, 1978, 1983) are integrated to estimate the advection aridity model evapotranspiration in Sardon, Spain.

1.2. General Objective

The general objective of this research is to validate the actual evapotranspiration by the Advection Aridity method using ground based measurements.

Specific Objectives

1. To investigate the proper wind function to run the Advection Aridity model.
2. To evaluate the accuracy of the AA model during relatively wet and dry condition.
3. To evaluate effect of the temporal resolution on the accuracy of the model

1.3. Research Questions

1. What is the accuracy of Advection Aridity Approach in Sardon, Spain?
2. Which environmental condition the Advection Aridity model estimates more effectively, in relatively wet or dry?

1.4. Research Output

The outputs of this study are:

1. An assessment of meteorological parameters in the study area and an analysis of their impact on energy balance.
2. The best choice for the wind function over Ethiopia
3. The AA model output of half hourly and daily for both wet and dry condition.
4. Comparison and accuracy assessment of the AA model output using eddy correlation measured ET for both half hourly and daily.

1.5. Structure of the Thesis

In Chapter 2, the theoretical background of the advection aridity model and proposed formulation of wind functions. **In Chapter 3**, study area and measurement instruments. **In Chapter 4**, the methodology, and data processing are described. In this chapter the methodology is focussed on advection aridity model and its respect to three wind functions: standard measured and calibrated. **In Chapter 5**, the results and discussion are described. Special focus lies on the results, half hourly and daily of the aridity model result in comparison with eddy correlation measured evapotranspiration. In this chapter also an accuracy assessment is described by the complementary relationship of the normalized ET which evaluates the principle of the advection aridity proposed by Bouchet's (1963). **In Chapter 5**, the main result of the thesis summarized into conclusion and recommendation.

2. THEORETICAL BACKGROUND

2.1. Introduction

Knowledge on the hydrological cycle has and especially the role of the evaporation component has been developing for a long time (Brutsaert, 1982). The first quantitative measurements of evaporation generally were already performed in the 17th century and are attributed to Edmund Halley (see Brutsaert, 2005). However, it was John Dalton, a scientist living in the north of England between 1766 and 1844 (Gash & Shuttleworth, 2007) who was the first to understand the fundamentals of the process of evaporation. Dalton realized that water vapour existed in the atmosphere as a separate entity and the amount of water stored in the atmosphere could increase with temperature (Gash & Shuttleworth, 2007).

Expressing this as an equation would give evaporation, E , as:

$$E = K(e_s - e_a) \quad (2-1)$$

Where K is a wind speed – dependent coefficient e_s is the saturated vapour pressure at the water temperature and e_a is the vapour pressure of the air above. This basic equation eventually led to the formulation adopted by Penman (Penman, 1948) and forms the basis for modern physically – based models of evaporation (Brutsaert, 1982; Gash & Shuttleworth, 2007).

An evaporating soil or a transpiring plant surface is a dynamic system interacting constantly with the atmosphere and the interior of the soil. The transfer of energy from the soil/plant surface occurs in terms of sensible heat and heat of vaporization to the atmosphere and by the process of conduction to the soil (Haque, 2003). As for large scales the soil and plant cannot be distinguished these processes are combined into evapotranspiration. Several evapotranspiration are identified: (1) the equilibrium evapotranspiration which is controlled only by the available of energy (and thus representing an lower limit to evapotranspiration); (2) the wet – surface evapotranspiration which is controlled by the available energy and atmospheric conditions and the saturation vapour pressure at the actual surface temperature (and thus represents an upper limit to evapotranspiration); and (3) the actual evapotranspiration ET_a , which is the amount of water atmosphere under a given energy and climatic conditions (Haque, 2003).

Estimation of actual evapotranspiration has been proposed in literature in several methods. These methods can be divided in terms of complexity (Glenn et al., 2007) (Kalma et al., 2008), from simple empirical methods, to more difficult energy balance methods, like the Surface Energy Balance Algorithm for Land (SEBAL) (Bastiaanssen et al., 1998), the Surface Energy Balance System (SEBS) (Su, 2002) and the Two Source Energy Balance (TSEB) (Kustas & Norman, 2000) extremely complex Land surface models (GLDAS, ECMWF). In this research only the simple empirical models are investigated as in the other methods input variables are required that are not measured in Ethiopia.

Most simple methods are based on the work of (Monteith, 1965) and Penman (1948). These introduced resistance terms and derived at an equation for evapotranspiration from surfaces with either optimal or limited water supply. The combination of those works, often referred to as Penman–Monteith method, has been successfully used to estimate evapotranspiration from different land covers. However the method requires data on aerodynamic resistance and surface resistance which are not readily available. Consequently the Penman–Monteith method for estimating actual evapotranspiration has been limited in practical use (C. Y. Xu & Singh, 2005). The complementary relationship proposed by Bouchet (1963) however circumvents this. For the areal evapotranspiration estimation, this method is usually preferred because it requires only standard meteorological variables. Based on complementary relationship concept, different models have been derived, which include the advection–aridity (AA) model proposed by

Brutsaert (1979), the complementary relationship areal evapotranspiration (CRAE) model derived by Morton (1978, 1983), and the complementary relationship model proposed by Granger and Gray (1990) using the concept of relative evapotranspiration (the ratio of actual to Potential evapotranspiration).

2.2. Complementary Relationships

Bouchet's hypothesis of a complementary relationship (1963) states that in a certain areas, there exists a complementary feedback mechanism between actual (ET_a) and potential (ET_p) evapotranspiration. Potential evapotranspiration is the amount of evaporation that would occur if a sufficient water source were available. Actual evapotranspiration is considered the net result of atmospheric demand for moisture from a surface and the ability of the surface to supply moisture, and then ET_p is a measure of the demand side. The hypothesis states that when water availability becomes limited (under conditions of constant energy input to a given land surface-atmosphere system), this, then the energy excess (in the form of sensible heat and/or long wave emitted-radiation) increases the temperature and humidity gradients of the atmosphere; this in turn leads to an increase in ET_p in magnitude to the decrease in ET_a .

In this context, ET_p is defined as the evapotranspiration that would take place from a moist surface limited only by the amount of available energy. The reference evapotranspiration (ET_{po}) rate would occur if the surface was brought to saturation (Parlange & Katul, 1992). Under the conditions where ET_a is equal to ET_p , this rate is referred to as the wet environmental evapotranspiration. When the water for evapotranspiration becomes limited at the surface the complimentary relationship will be decrease (for the same quantity of energy available),

$$ET_a - ET_{po} = -q_1 \quad (2-2)$$

So that q_1 becomes the available energy which increases the potential ET. A decrease in ET_a to values below ET_{po} affects primarily the air temperature, the air humidity, and the stability of the atmosphere (Bouchet's, 1963). Bouchet's then hypothesized that the change in the ET_p could be given by:

$$ET_p = q_1 + ET_{po} \quad (2-3)$$

While in the original derivative (2-2), Bouchet's (1963) assumed that in [eq (2-3)] ET_p increased by exactly q_1 ; using the combination of [eq (2-2)] and [eq (2-3)] immediately yields the simple complementary relationship as follows:

$$ET_a + ET_p = 2ET_{po} \quad (2-4)$$

Where: q_1 does not alter the available energy (Parlange & Katul, 1992). The main assumption behind the complementary relationship is that the energy released by the decrease in areal evapotranspiration compensates exactly the increase in potential evapotranspiration. Potential ET, a concept introduced by Thornthwaite (1948), refers to the rate of evaporation from a large area covered completely and uniformly by an actively growing vegetation with water available as needed. A widely used standard for potential ET is originally based on Penman (1948, 1956) equation. The concept of a complementary relationship between actual ET and potential ET originally developed by Bouchet's (1963) and subsequently developed by others (Morton, 1976, 1978) is the bases of Brutsaert (1979) models.

2.3. Potential Evapotranspiration(Penman model)

Today widely used standard for potential ET is based on equation of Penman (1948). The Penman (1948) was one of the earliest hydrologists to depict evaporation in terms of two main micrometeorological components: energy for the conversion of water to a vapour and aerodynamic process for the removal of saturated air away from the surface (X. Xu & Li, 2003) . The Penman equation is thereby widely known as the combined equation model for estimating evaporation. It was developed originally to estimate the potential evaporation of water and saturated land surfaces. The familiar expression of the Penman equation for ET_p is usually expressed as:

$$ET_p = \frac{\Delta}{\Delta + \gamma} Q_{ne} + \frac{\gamma}{\Delta + \gamma} E_a \quad (2-5)$$

Where Penman's (1948) originally derivation it was assumed that Q_{ne} is the energy in $W m^{-2}$, Δ is the slope of the saturation vapour pressure curve at air temperature in $kPa \text{ } ^\circ C^{-1}$, γ is psychrometric constant is in $kPa \text{ } ^\circ C^{-1}$ and E_a is the drying power of the air. The drying power and psychrometric constant, calculated according to Brutsaert (2005), are shown in the following equations.

$$E_a = f(u)(e_s - e_a) \quad (2-6)$$

$$\gamma = \left(\frac{c_p P}{0.622 \lambda} \right) \quad (2-7)$$

With $f(u)$ the wind function, and $\lambda = 2.501 - 2.361.T.10^{-3} [MJ kg^{-1}]$ is latent heat of vaporization, C_p is specific heat in $M J kg^{-1} \text{ } ^\circ C^{-1}$, P is atmospheric pressure. At the moment there is no single parameterization for the wind function. More information on this wind function will be provided paragraph 2.5.

2.3.1. Wet Evapotranspiration

The two term of structure of Penman (1948) [eq (2-5)] may serve as an aid in understanding the effect of advection. When the air has been in contact with a wet surface over a very long fetch, it could be argued that it may tend to become vapour saturated, so that E_a , shown in [eq (2-5)], should tend to zero (Brutsaert, 2005). Accordingly, Slatyer and Mollory (1961) reasoned that the first term on the right of [eq (2-5)] may be considered a lower limit for evaporation from moist surfaces, as is shown in the following equation

$$E_e = \frac{\Delta}{\Delta + \gamma} Q_{ne} \quad (2-8)$$

Here (E_e) is referred to as the equilibrium evaporation. Consequently the second term of [eq (2-5)] may be interpreted a departure from that equilibrium (Brutsaert, 2005).

Later Priestley and Taylor (1972) used the equilibrium evaporation as the basis for an empirical relationship to describe evaporation from a wet surface under conditions of minimum advection, ET_{po} ; they analyzed data obtained over ocean and saturated land surfaces in terms of α , defined by $ET_{po} = \alpha E_e$. The wet surface evapotranspiration (ET_{po}), and is controlled by available energy and atmospheric conditions. Thus:

$$ET_{po} = \alpha \frac{\Delta}{\Delta + \gamma} (R_n - G_o) \quad (2-9)$$

Where, R_n is net radiation (W m^{-2}), and G_o is the ground heat flux (W m^{-2}). Priestley and Taylor (1972) decided that for large saturated land and what they termed 'advection-free' water surface best estimate is $\alpha = 1.26$, and supposed to describe evaporation from an extensive saturated surface with minimal advection.

2.4. Aridity Advection Model and Proposed Formulations

The Brutsaert (1979) Aridity Advection (AA) model and proposed formulation is based on the complementary relationship given by [eq 2-4]. Brutsaert (1979) proposed the use of the Priestley – Taylor (1972) model to estimate ET_{po} , and Penman (1948) for ET_p . They found by substitution of the complementary relationship [eq (2-5)] (with ground heat flux included) and Priestley-Taylor (1972) [eq (2-9)] into [eq (2-4)] the following equation for ET_a .

$$ET_a = (2\alpha - 1) \frac{\Delta}{\Delta + \gamma} (R_n - G_o) - \frac{\gamma}{\Delta + \gamma} E_a \quad (2-6)$$

Where: ET_a is aridity advection model evapotranspiration (W m^{-2})

2.5. Wind Function and AA model

Wind function examined based on under neutral condition - i.e. a stable atmospheric boundary layer. For the neutral is the mass transfer wind coefficient used. Under empirical is the Penman (1948) and calibrated wind function used. As Brutsaert (1979) stated in hydrological practice there is still no universally accepted way to calculate $f(u)$, the wind function in E_a , which is the drying power of the air as defined in [eq (2-6)].

2.5.1. Penman wind function and AA model

The general type of wind function was proposed by Stelling in 1822 (see Brutsaert, 1982), and still in use today, can be written as

$$f(u) = (a + b \cdot \bar{u}) \quad (2-11)$$

The introduction of the additional constant, a , in [eq (2-11)] is viewed as a means of improving the fit between the mean wind speed and the rate of evaporation (Brutsaert, 2005). Penman (1948) estimated the mass transfer coefficient empirically to be $a = 0.26$ and $b = 0.26 \cdot 0.54$, resulting in

$$f(u) = 0.26(1 + 0.54 \cdot \bar{u}) \quad (2-7)$$

Where \bar{u} is the mean wind speed in m s^{-1} and the constants requires that in [eq (2-12)] is in mm/day and the vapour pressure in hPa . Substituting the Penman wind function of [eq (2-12)] into AA model [eq (2-10)], creates the following:

$$ET_a = (2\alpha - 1) \frac{\Delta}{\Delta + \gamma} (R_n - G_o) - \frac{\gamma}{\Delta + \gamma} \left(0.26 \left(1 + 0.54 \cdot \bar{u} \right) \right) (e_s - e_a) \quad (2-8)$$

This is called the AA model with integrated Penman wind function. In this study we called this the standard wind function in advection aridity (AA) model.

2.5.2. Wind function in neutral atmosphere and AA model

In Brutsaert (2005), the drying power of evaporation in terms of mass transfer coefficient is expressed as follows:

$$E_a = C_e \cdot u \cdot \rho \cdot (e_s - e_a) \quad (2-9)$$

Where C_e is the mass transfer coefficient which is given by Brutsaert (2005):

$$C_e = \frac{k^2}{\ln[(z_2 - d_o) / z_{ov}] \ln[(z_1 - d_o) / z_o]} \quad (2-10)$$

If $z_2 = z_1 = z_{ov}$, this equation can be simplified to

$$C_e = \frac{k^2}{\ln[(z - d_o) / z_o]^2} \quad (2-11)$$

Brutsaert (2005) explained that under neutral atmospheric conditions the concentration of any admixture of the flow is a logarithmic function of height above the ground. Brutsaert states that in plan-parallel flow an increase in velocity the z- direction is evidence of a sink at the surface. Thus, the mean velocity gradient in a fluid of density is determined by the shear stress at the wall, and the distance from the wall, (z-do). The last variable, the zero – plane displacement height do is introduced to account for the uncertainty of the position of the wall in the case of irregular and uneven surfaces. These variables can be combined into a single dimensionless quantity as follows:

$$\frac{u_*}{(z - do)(du/dz)} = k \quad (2-12)$$

Where, u and u_* are the velocity and the friction velocity [$m s^{-1}$] and k is the von Karman's constant. The solution of this differential equation is a logarithmic profile, which is written as

$$\bar{u} = \frac{u_*}{k} \ln\left(\frac{z - do}{z_o}\right) \quad (2-13)$$

Where, z_o integration constant [m], and is usually referred to as the momentum roughness length. This equation can thus be used to simplify the C_e into
Gives

$$C_e = \left(\frac{u_*}{u}\right)^2 \quad (2-14)$$

Van der Tol et al. (2003) used this simplified transfer coefficient for Penman aerodynamic conductance, substituting the simplified mass transfer coefficient into the drying power of ET for the study area expressed as follows:

$$ET_a = (2\alpha - 1) \frac{\Delta}{\Delta + \gamma} (R_n - G_0) - \frac{\gamma}{\Delta + \gamma} \left(\frac{u^*}{u}\right)^2 u \cdot \rho \cdot (e_s - e_a) \quad (2-15)$$

This is called the measured wind function in the advection aridity model

2.5.3. Calibrated wind function

The third applied wind function that was tested was the empirically calibrated wind function (Morton, 1978, 1983). Under calibration the suitable constant values are represented to optimize the daily model output accuracy.

$$f(u) = A(B + C \cdot u) \quad (2-21)$$

Where, A (3.918), B (1.186) and C (0.2). The Priestley – Taylor (1972) proposed the mean are empirical coefficients under minimal advection $\alpha = 1.26$, Brutsaert (1982) proposed that $\alpha = 1.26$ to 1.28 for short vegetation and open water surfaces. Hobbins et al (2001b) adopted a value of $\alpha = 1.28$ to estimate regional evapotranspiration across the conterminous USA. Lemeur and Zhang (1990) and Liu and Kotoda (1998) used a value of $\alpha = 1.26$ river basin in western China respectively. Zhang et al. (2004) found that the seasonal average α is 1.17 and 1.26 for winter wheat and 1.06 and 1.09 for maize in the North China Plain. This indicates that the value of α could be different for different season, In this paper for the advection aridity model the value of alpha = 1.06 for dry condition and 1.267 for wet condition is adopted The value of the Priestley – Taylor coefficient α has been the subject of much discussion for various land- cover types and at a range of temporal scales (Hobbins et al., 2001b) Brutsaert (1979) shows that the exact value of $\alpha = 1.26$ was probably not very sensitive to the AA model. Moreover, under or over estimation of AA model is removed by recalibration of wetter ET, α (Hobbins et al., 2001).

The same as standard and measured wind function; it was validated with measured ET and complementary relationship.

2.6. Normalized Evapotranspiration

The normalized evapotranspiration relationship is used to show the trends of Bouchet's (1963) assumption (see section 2.2). Here both ET_a and ET_p are normalized with the true potential evaporation (ET_{po}).

The moisture index (x-axis) is within the range of 0 to 1. Where, 0 is the normalized ET(y – axis) for a value of maximum potential and least actual ET (very dry condition). When the normalized ET is equals to one, the actual ET equals potential (wetted environment) ET.

$$\frac{ET_a}{ET_{po}} = \frac{2ET_a / ET_p}{1 + ET_a / ET_p} \quad (2-22)$$

$$\frac{ET_p}{ET_{po}} = \frac{2}{1 + ET_a / ET_p} \quad (2-23)$$

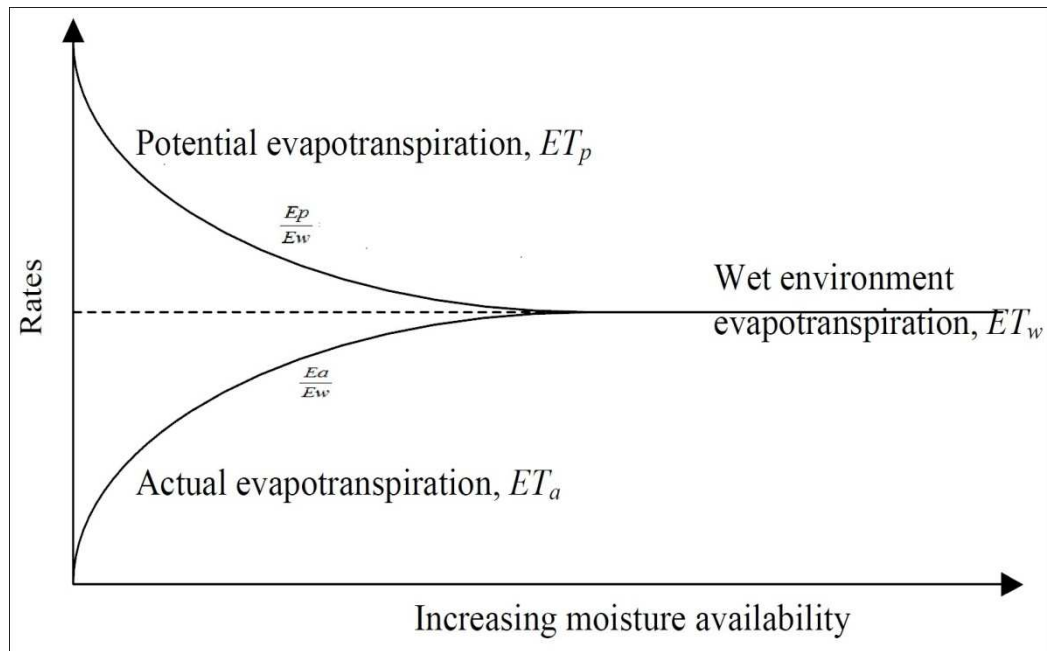


Figure 2-1 : Sketch illustrates the complementary relationship between the ET_a and ET_p for varying moisture condition in terms of moisture index, ET_a/ET_{p0} .

3. STUDY AREA

This research was done in Sardon, Spain. The Sardon Catchment is located in the central–western part of Spain, in the Salamanca province between the geographic coordinates of $6^{\circ}07'$ - $6^{\circ}13'$ W longitudes and $41^{\circ}01'$ - $41^{\circ}08'$ N latitudes. The Sardon area is part of the Rio Tames catchment whose major tributary is Sardon River. The Sardon catchment is more elongated towards North-South direction having total area of approximately 80km². The study area is shown in below Figure 3-1

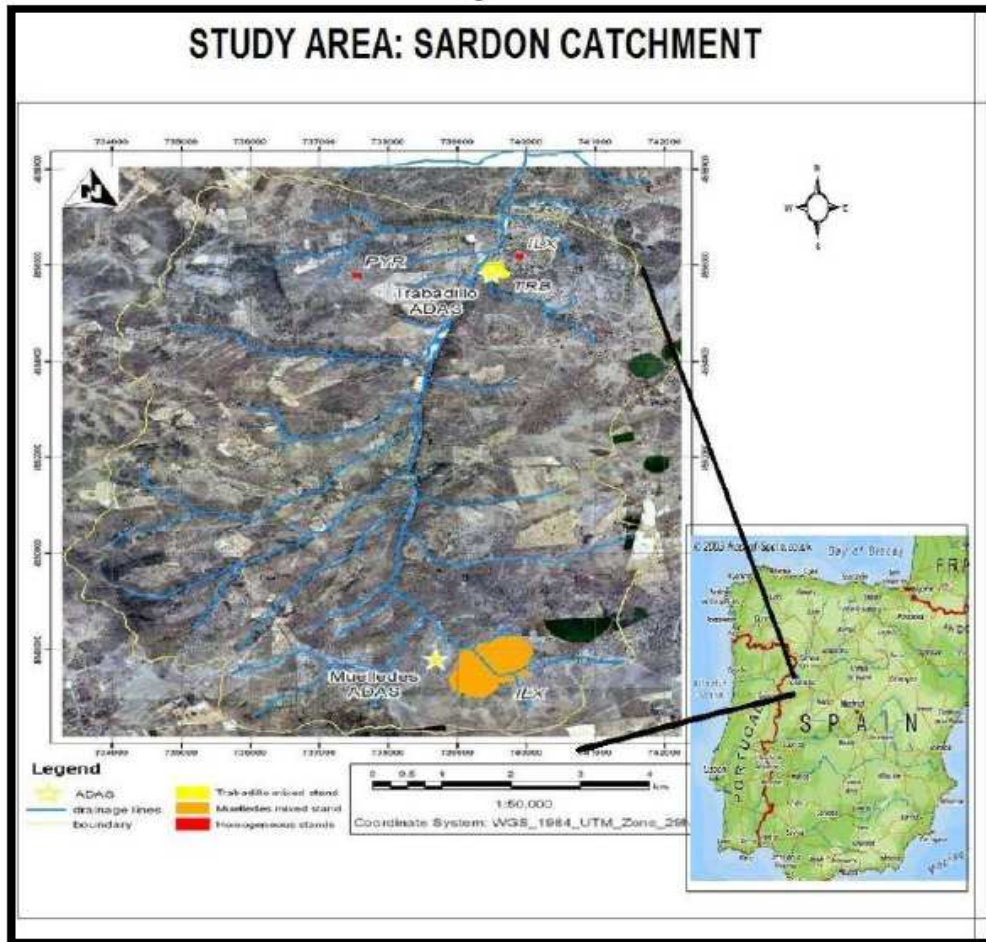


Figure 3-1 : Map of the Study area

The climate in the study area is semi-arid, with potential evapotranspiration (ET_p) is on average 5mm/d and rainfall is less than 20mm/month (Lubczynski & Gurwin, 2005). The long term 23 years mean rainfall is approximately 500mm/yr. The warmest and driest month in the study area are July and August when the average temperature is about 22°, see

The land cover in the study area is characterized by natural woody-shrub vegetation. The area is used mainly for pasture because the soil contain large proportion of weathered granite, which make them generally unsuitable for agriculture. There are only two types of tree species in the study area: evergreen oak *Quercus ilex* and broad- leafed deciduous oak *Quercus Pyrenaica* (Lubczynski & Gurwin, 2005).

A detail description of the area can be found in the work of Lubczynski and Gurwin (2005), Ontiveros Enriquez (2009), Ruwan Rajapakse (2009) and Rwasoka (2010).

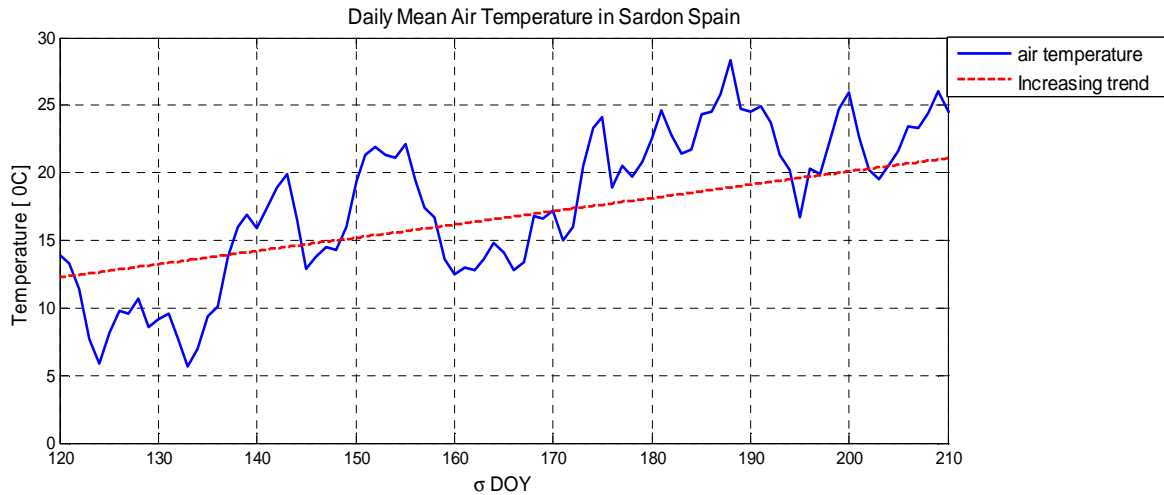


Figure 3-2 : Daily mean air temperature from 120-210 Julian days in 2010

3.1. The Data and Measuring Instrument

The data used in this study came from eddy correlation tower which was erected in Trabadillo, Spain in July 2009. On this tower a variety of instruments is installed.

- The turbulence measurement was made using a CSAT-3 (Campbell scientific, USA) 3-D sonic anemometer. The CSAT-3 measures sonic temperature (T_s) and the stream wise, cross-wind and vertical wind speeds, u_x , v_y and w_z respectively. The measurements are made using pairs of 3 orthogonally oriented transducers over a path that is vertically 10 cm long and horizontally 5.8 cm wide.
- In combination with the LICOR L1 7500(Lico Inc, USA) one-path CO_2/H_2O infrared gas analyzer, the fluxes from the land surface can be measured at high temporal resolution.
- The net radiation budget components were measured using a CNR 1 Net Radiometer (Kippa and Zonen, Delft, Netherlands). The CNR 1 Net Radiometer measures: shortwave incoming, shortwave outgoing, long wave incoming and long wave outgoing radiation separately through upward and downward facing pyranometers and pyrgeometers.
- Licor. Soil heat flux was measured using Hukseflux soil heat flux plates. Two of the plates were buried at the depth of 1 cm and the other one at 10 cm depth. The deeper one was used in a different soil heat flux calculation that included heat storage changes monitored with two TCAV-L averaging soil thermocouple probes is at 2 and 7 cm depth. Each TCAV-L sensor consists of three smaller sensors, from which the average temperature is recorded. .
- The Vaisala weather transmitter WXT520 (Vaisala, Finland) used to measure the meteorological variables (aligned to the north). The instruments measures: relative humidity (RH), rainfall (duration and intensity), air pressure, air temperature, wind direction and speed.



Figure 3-3 : a) To the left side is CSAT-3(Campbell Scientific, 1996) and CO₂/H₂O gas analyser LICOR L1 7500, b) to the right side includes all CSAT-3, CNR 1 Net Radiometer (Kipp & Zonen) and Vaisala in eddy tower Sardon, Spain.

4. METHODS

The three wind functions have three different advection aridity model outputs. The result validated based on, 1) by comparison with eddy tower measured ET, 2) by the complementary relationship between actual and potential evapotranspiration which is the basic concept proposed by Bouchet's (1963) in the formulation of AA model.

In this research ET is estimated by the Advection Aridity (AA) model. The model calculates evapotranspiration on basis of the drying power of the air, characterized by a wind function. Three different wind functions are tested:

- a. AAs: Standard (Penman, 1948). Penman (1948) formulated the wind function based on an empirical relationship shown in the methods we applied those empirical constants into the AA model (see section 2.5.1)
- b. AAm: Transfer (relating with measured data). Such a wind function first Proposed by Thom (1975) and then by Van der Tol et al (2003) for aerodynamic conductance of Penman – Monteith equation (Monteith, 1965). The empirical simplification of the equation is presented in Chapter two theoretical sections 2.5.2
- c. AAc: Empirically calibrated wind function (Morton, 1978, 1983). The method of extracting the calibrated wind function is shown Table 4-1 and section 2.5.3

Table 4-1 illustrated the wind function of standard, measured and empirically calibrated. In the measured the term u_*/u was derived by a regression of the observed u_* against u . The calibrated constants determined by both programming on Matlab software looking for the least mean square error and manually by trial and error in order to keep the basic principle of complementary relationship.

Table 4-1 : Illustrates the three wind function integrated in the advection aridity model (AA model) and its product of model output

Model	wind function	wind function equation	model result
	standard	$f(u) = 0.26(1 + 0.54.u)$	half hourly, daily
AA* model	measured	$f(u) = \left(\frac{u_*}{u}\right)^2 .u.\rho$	half hourly, daily
	empirically calibrated	$f(u) = A(B + C.u)$	daily

- AA* advection aridity model

4.1. Methodology frame work

The flowchart of the methodology is shown in Figure 4-1. The ET outputs of these three methods are evaluated by comparing them with measured ET, and are summarized in to conclusion and recommendation. In specific the focus of this research was for wet and dry condition.

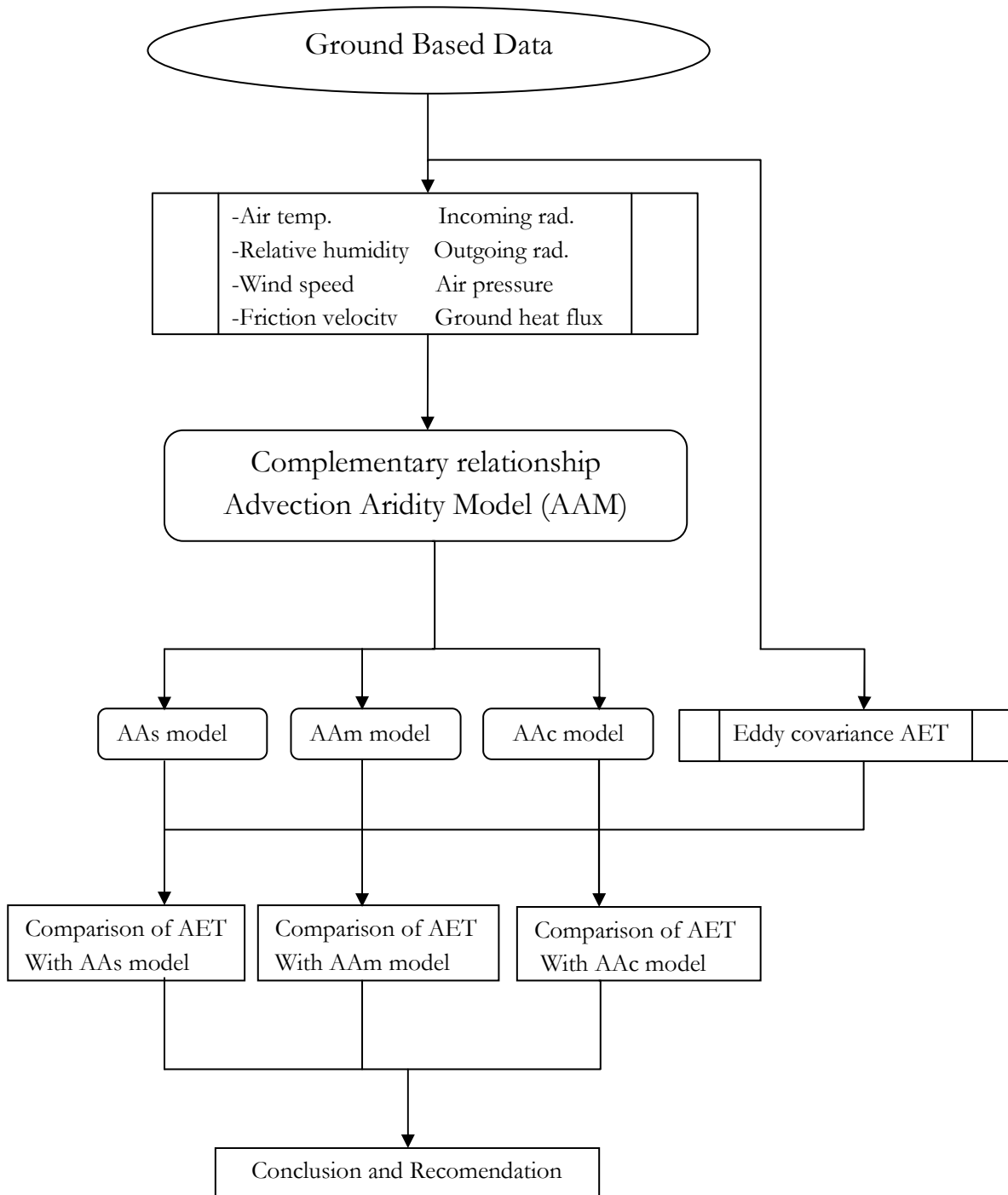


Figure 4-1 : Methodology flow chart

- AAAs : is advection aridity model with standard wind function
- AAM : is advection aridity model with measured wind function
- AAc : is advection aridity model with calibrated wind function

4.1.1. Comparison Interpretation of data

The complementary relationship (CR) is one way for the validation of the model ET. This CR method is explained in Chapter two theoretical sections 2.2 and 2.6 According to the complementary relations ship, the compensation trend between actual ET and potential ET was evaluated both for half hourly and daily AA model output. Using the statistical analysis the AA model compared with measured eddy tower. For example, how the models result correlated, and error from actual measured ET. The statics which was applied mean, maximum, correlation, coefficient of determination, and root mean square errors (RMSE). Finally the result was interpreted statistically in combination with complementary relation trend.

4.2. Data Set

The AA model requires the following data: air temperature, pressure, relative humidity, wind speed, friction velocity, incoming long wave radiation, incoming shortwave radiation, outgoing long wave radiation, outgoing long wave radiation and ground heat flux. The data which used for this research was from March to September, 2010.

For our validation we required the following data: eddy tower measured latent heat flux and in the data set the major work divided into pre – processing, processing and post processing.

4.2.1. Pre-processing

One of the challenges for analysis of the AA model is no specific software that could apply to it. Pre - processing of raw data was performed such as Matlab software could be used to program the AA model. During the field work the data gained from the Campbell Scientific CR5000 data logger in a digital form, back up by pc card reader and its capacity is about 2 GB. The data logger programmed to download in a digital form of every five minute. This data was converted into numerical value, processing of the flux data and a quality control was performed by the AltEddy processing software. Afterwards the data was converted to meteorological parameters variables, incoming and outgoing radiation fluxes (see Table 4-2). The filtered data was written to ASCII format for the standard meteorological data and 30-minutes for the fluxes. From these amount data, the months with minimum of missing data that includes dry and wet conditions were used before pre-processing.

Table 4-2 : Pre-processed data. The parameter used in the model for both half hourly and daily

Ground based data	Units
Air temperature	°C
Pressure	hPa
Wind speed	m s ⁻¹
Relative humidity	%
Rainfall	mm
Friction velocity	m s ⁻¹
Soil temperature at 2 cm	°C
Soil temperature at 7 cm	°C
Incoming short wave	W m ⁻²
Incoming long wave	W m ⁻²
Outgoing shortwave	W m ⁻²
Outgoing long wave	W m ⁻²
Sensible heat flux	W m ⁻²
Latent heat flux	W m ⁻²
Soil heat flux at 1 cm	W m ⁻²

Soil heat flux at 10 cm	$W m^{-2}$
-------------------------	------------

Table 4-3 : Processed product from the meteorological parameter and available energy

Processed products	Units
Saturated vapour pressure(FAO & Mean)	kPa
Saturated vapour deficit(FAO & Mean)	kPa
Actual vapour pressure(FAO & Mean)	kPa
Slope of saturated vapour pressure(FAO & Mean)	$kPa\ ^{\circ}C^{-1}$
Latent heat of vaporization	$MJ\ kg^{-1}$
Surface heat flux	$W\ m^{-2}$
Net radiation	$W\ m^{-2}$
Energy balance closure	$W\ m^{-2}$
Potential ET	mm /day
Wetted ET	mm /day
Actual ET	mm /day

4.2.2. Processing of data

Among the pre-processed and processed analyzed equation includes; energy balance equation, derived meteorological parameter equation, for example, mean saturated vapour pressure and slope of saturated vapour pressure. Those daily derived meteorological parameter were exempted by two methods: 1) by using daily mean value of each parameter, 2) by FAO No. 56 mean methods (the mean is average of daily maximum plus daily minimum) (see section 4.3.5). Comparing the preceding result (between daily mean and FAO No. 56 mean), the best representative of daily mean methods was implemented for the post-processing model equation. The AA method applied to both half hourly and daily average data, but the FAO method is useful because in other places like Africa only T_{min} and T_{max} are available

4.2.3. Post - Processing of data

In the post-processing, every data which were previously organized in the pre-processing and processing, were applied to the final AA model equation. Moreover, parameter and constants like available of energy for evaporation, and Priestley-Taylor coefficient were used. By using Matlab code programming, regression analysis and calibration, those three wind function AA model result for both half hourly and daily evaluated.

4.3. Meteorological Parameter

Meteorological variables are the main input of AA models. In the following sub sections the input and its processing is analyzed. This was analyzed based on FAO No. 56. The FAO No 56 uses the standard climatic data that can be easily measured or derived from commonly measured data. For instance, meteorological variable products (relative humidity, wind speed, air temperature, actual vapour pressure), which is available in most meteorological weather station. The meteorological variables can be expressed in several units, but here in the study parameter used units was the one which required to the advection aridity model as parameter input unit.

4.3.1. Meteorological Data Quality Control

The first requirement before put data into analysis was quality control. The meteorological data, which was measured by the instrument of Vaisala quality control analysis. The meteorological parameters used for model analysis are Temperature, wind speed and direction, relative humidity and pressure. Meanwhile as quality control analyzed, the product of standard meteorological parameter like saturated vapour pressure and actual vapour pressured are derived.

4.3.2. Mean Saturated Vapour Pressure

The calculation of saturation vapour pressure in terms of air temperature expresses by:

$$e_s = 0.6108 \exp \left[\frac{17.27T}{T + 237.3} \right] \quad (4-1)$$

Where e_s is the saturation vapour pressure [k pa], and T is air temperature [°C].

The saturation vapour pressure is a function of air temperature, see Table 4-4. These values were calculated using the eddy tower data at different Julian days of 33, 67,103, 150, 184, 229, 233 and 237. As the temperature increases, the saturation vapour pressure and slope of saturation increases but the latent heat of vaporization decreases. At low temperatures compared with high, the slope was small and varies only slightly as the temperature rises. Wet condition temperature decreases below -5°C and results its vapour pressure to decreases below 0.5 hPa. In dry conditions, the temperature increases to values over 30 °C consequently its vapour pressure increases more than 4.5 hPa, too. These two seasons' data analysis shows a net difference of 4 hPa. Thus, due to season change, the saturation vapour pressure affects on the advection aridity model ET estimation.

Table 4-4 : Some more properties of water vapour in Sardon

<i>DOY</i>	<i>Temperature(°C)</i>	<i>Le(M J kg -1)</i>	<i>e(hpa)</i>	$\Delta(hPac - 1)$	$\left(\frac{\gamma}{\Delta}\right)$
33	-5	2.498	0.41	0.031	1.95
67	-1	2.497	0.57	0.042	1.44
103	5	2.479	0.87	0.061	1.00
150	11	2.455	1.28	0.086	0.72
184	15	2.449	1.72	0.111	0.56
229	19	2.443	2.21	0.138	0.45
233	26	2.437	3.27	0.194	0.24
237	31	2.427	4.49	0.255	0.22

Le: latent heat of vaporization; e: saturation vapour pressure Δ : slope of saturation vapour pressure.

4.3.3. Actual Vapour Pressure

The actual vapour pressure is the vapour pressure exerted by the water in the air. When the air is not saturated, the actual vapour pressure will be lower than the saturation vapour pressure.

The actual vapour pressure is derived from temperature and relative humidity. The calculation is expressed as follows:

$$e_a = 0.6108 \exp \left[\frac{17.27T}{T + 237.3} \right] \left[\frac{RH}{100} \right] \quad (4-2)$$

Where, RH is the relative humidity. As RH is 100 %(saturated) the actual vapour pressure and saturated vapour pressure are equal.

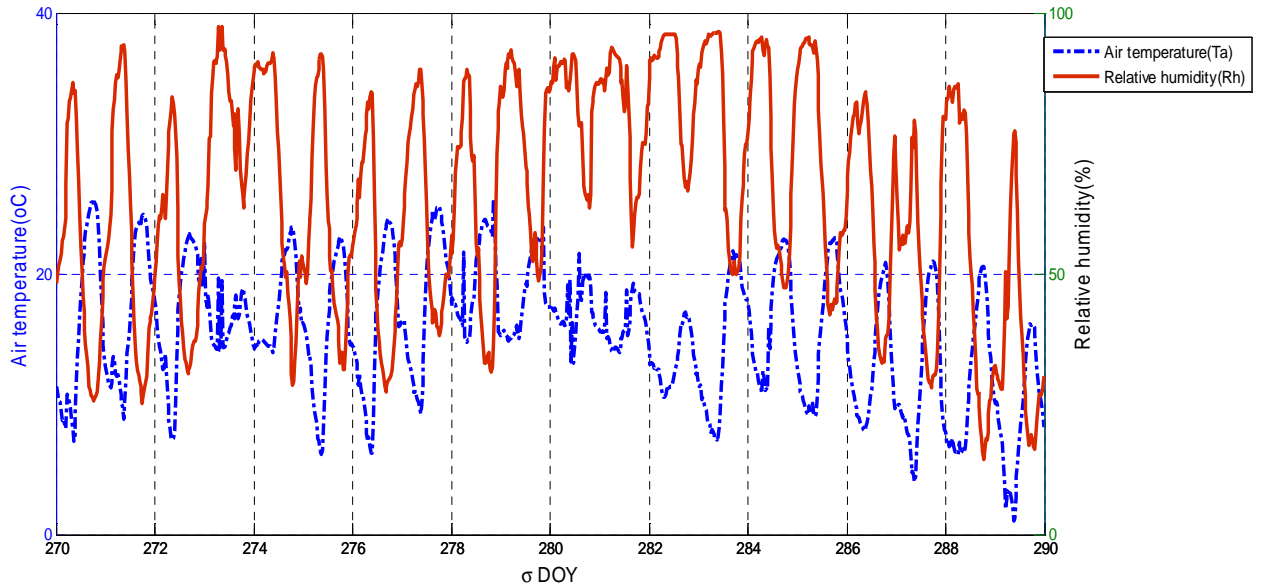


Figure 4-2 : Shows as temperature increases relative humidity decreases, inverse relationship between temperature and relative humidity.

4.3.4. Slope of Saturated Vapour Pressure

For the calculation of evapotranspiration by the model, the slope of the relationship between saturation vapour pressure and temperature is required.

$$\Delta = \frac{4098 \left(0.6108 \exp \left(\frac{17.27T}{T + 237.3} \right) \right)}{(T + 237.3)^2} \quad (4-3)$$

In the aridity advection model, the ratio between psychrometric constant and saturation vapour pressure causes in AA model estimation either to increase or decreases. Here at different sample temperature from Sardon catchment was taken to evaluate indirectly the influences of temperature on AA model ET. This sample temperature in (°C) was shown in Table 4-4: -5, -1, 11, 15, 19, 26 and 31°C. As temperature increases the ratio between psychrometric constant and saturation vapour pressure decreases, this ratio is the factor which multiplies the AA. This could also be one cause to increase the evaporation of the AA model if sufficient moisture is available.

4.3.5. Comparison of Daily Mean and FAO No.56 Daily mean of Meteorological Products

In analysis of processing to evaluate the mean for daily meteorological products, two methods examined one which was mentioned in FAO No 56, and another is the average of 30 minute data conversion into mean daily. For instance, FAO No 56 defines the mean air temperature as the mean of the daily maximum (Tmax) and minimum temperature (Tmin) rather than averaging the total daily observation, in this context we called it as mean method. These two mean methods of air temperature are input to derive meteorological products like slope of saturation vapour pressure. In Figure 4-3 shows that the result of

FAO No 56 mean and half hourly and daily mean slope of saturation vapour pressure. The result by FAO No 56 and by mean methods shows its R^2 is 0.98. As a result both methods are acceptable but the trend in FAO No 56 daily mean fluctuates more comparing to the daily mean for half hourly observation. For instance, on 272 DOY the FAO No 56 mean methods is lower than mean methods. In evaluating daily mean, only considering daily maximum and daily minimum may causes an error because this requires highly accurately filtered and measured data. The FAO No 56 methods are sensitive to have an error because the causes of error may be from calibration of instrument.

Moreover on day 274, FAO methods shown the mean value is higher than the value recoded on every 30 minutes of slope of saturation vapour pressure. Due to lot of observation data for the study area, the optimum accuracy and preferred methods for the analysis is 30 minutes mean methods.

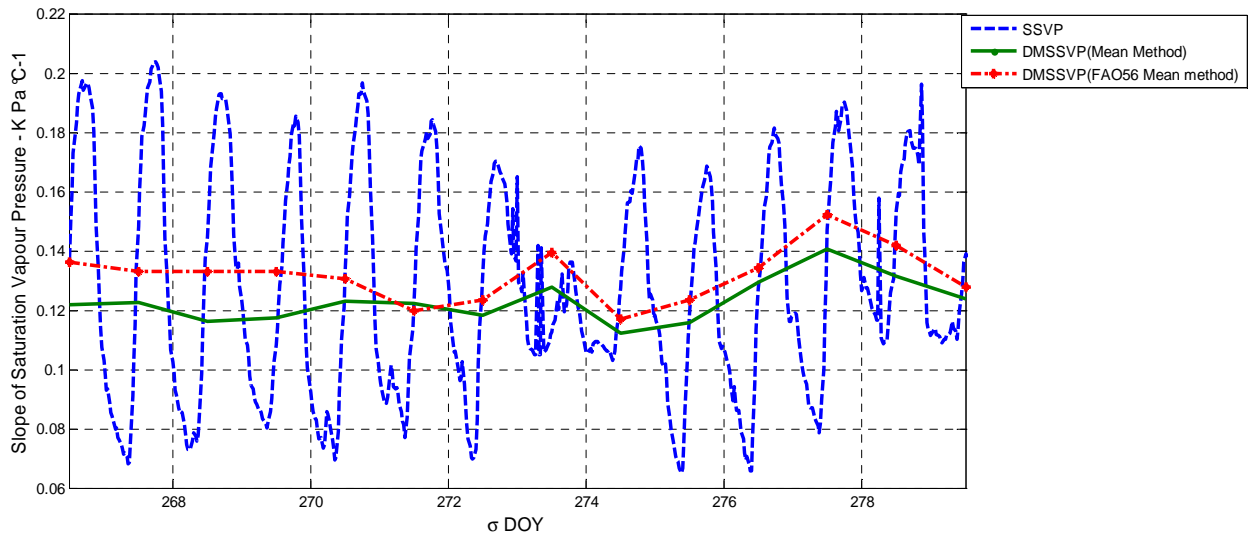


Figure 4-3 : Shows slope of saturated vapour pressure (SSVP) of 30 minutes, and daily mean slope saturated vapour pressure (DMSSVP) is for the mean method and FAO 56 mean methods

4.4. Net radiation

The Net Radiation (R_n) [Wm^{-2}] was determined as the balance of incoming and outgoing shortwave and long wave energy fluxes measured by the CNR 1 Net Radiometer (Kipp. & Zonen., 2002).the calculation is expressed as:

$$R_n = (SW \downarrow - SW \uparrow) + (LW \uparrow - LW \downarrow) \quad (4-4)$$

Where \uparrow indicates outgoing radiation and \downarrow incoming radiation and SW and LW refer to short wave and long wave radiation [$W m^{-2}$].

Figure 4-4 shows over DOY 266 – 269 energy component for the dry seasons. The sun's energy reaches in the study area of those days was $800 W m^{-2}$. The maximum net radiation was $400 W m^{-2}$.

The shortwave radiation reflected by the surface reached a maximum and a minimum of $211 W m^{-2}$ and $1.7 W m^{-2}$, respectively. The minimum value of 1 could be due to a calibration error as the expected minimum during night is zero.

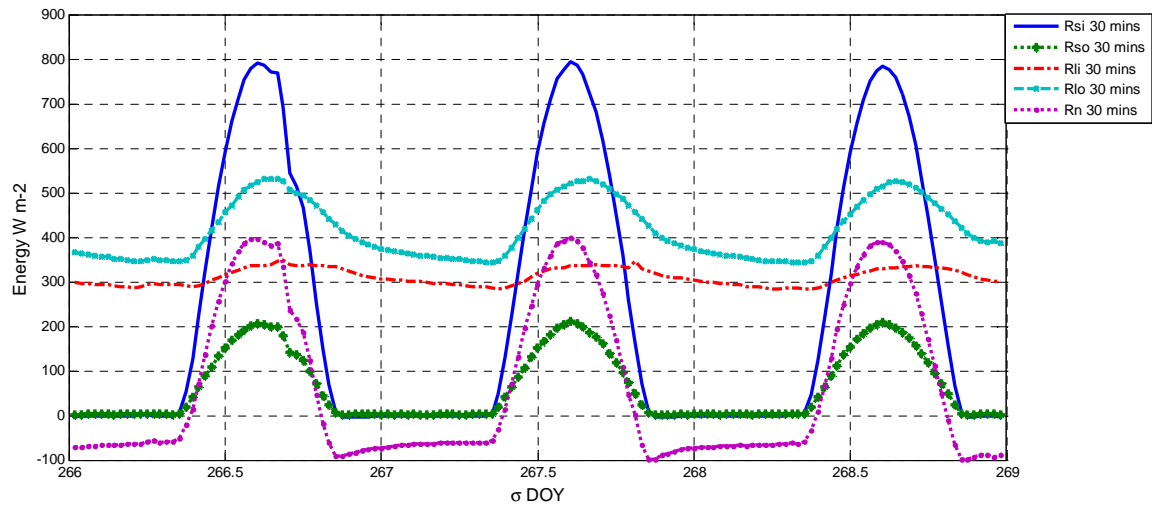


Figure 4-4 : Net Radiation Budget for three days of dry season

Table 4-5 analysis shows, the average net radiation constituted about 41 % of the average short wave incoming radiation and the rest partitioned to the other net radiation budget terms. During the dry period the maximum net radiation constitutes about 76% of the maximum observed incoming energy from the sun.

Table 4-5 : Illustrates a mean, minimum and maximum of radiation flux ($W m^{-2}$) in the study period 2010.

	Short Wave Incoming	Short Wave Outgoing	Long Wave Incoming	Long Wave Outgoing	Net Radiation
Average	257	58	317	410	106
Maximum	1022	237	425	633	780
Minimum	-5	-1	195	285	-119

4.5. Energy Balance

The energy balance equation used in the analysis was based on the measured net radiation, soil heat flux, sensible and latent heat flux, the equation is expressed as:

$$R_n = H + \lambda E + G_o \quad (4-5)$$

Where R_n is net radiation ($W m^{-2}$), H is sensible heat flux ($W m^{-2}$), λE is latent heat flux ($W m^{-2}$) and G_o is soil heat flux ($W m^{-2}$).

The energy balance closure was determined by plotting of the sum of sensible and latent heat fluxes against the available energy ($R_n - G_o$). The degree of energy balance closure determined by the line of 1:1 between $R_n - G_o$ and $H + \lambda E$.

Figure 4-5 shows the energy component of the study period during the influence of latent heat. In the influence of latent heat the Bowen ration $H/\lambda E$ indicates that the latent heat is 41 percent larger than sensible heat. The high latent heat and low sensible heat indicates that more evaporation in a wetted seasons. During the dry period, Donald (2010) analysis shown that the sensible heat flux is 43.7 percent larger than the measured latent heat flux

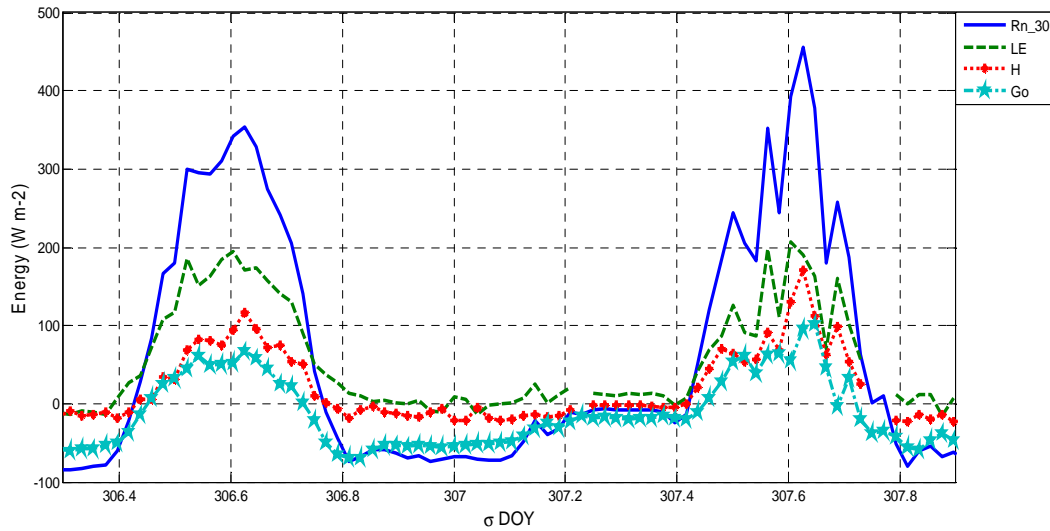


Figure 4-5 : Surface energy balance flux for DOY 306 – 308

Figure 4-6 shows the energy balance closure for both half hourly and daily. For half hourly the energy balance closure is 82% and for daily is 87 %. Both results are within the limit of expected energy balance closure 70 – 90 % (Twine et al., 2000). Taking into consideration of energy balance closure the collected data quality is good.

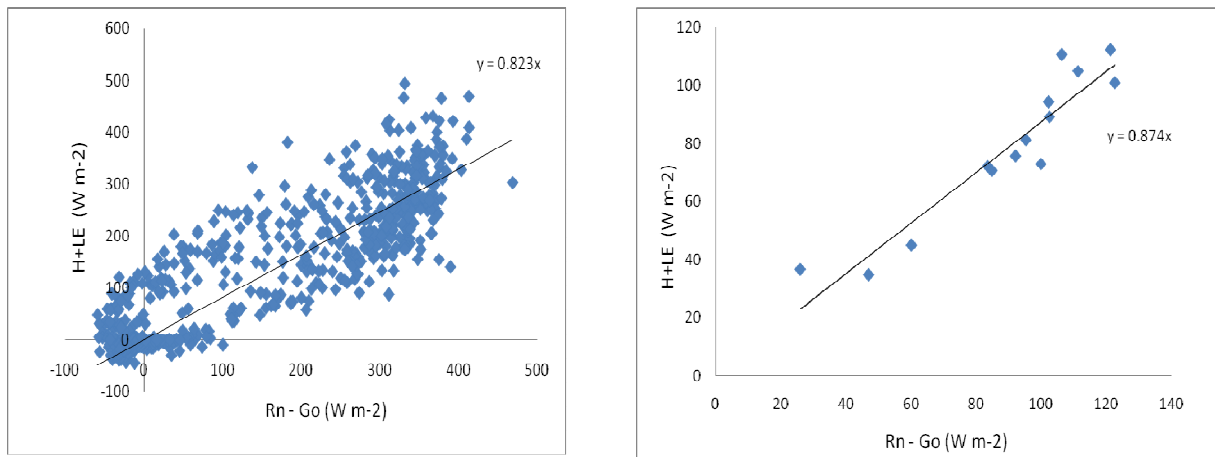


Figure 4-6: Energy balance closure: left side is half hourly and right side is daily energy balance closure. The x – axis is available energy ($Rn - Go$ storage) and on the y – axis is the sum of sensible and latent heat flux.

4.6. Evapotranspiration

Evapotranspiration was calculated from measured latent heat flux at 30 minute intervals. Firstly the latent heat of vaporization as a function of air temperature was determined as follows:

$$\lambda = 2.501 - 0.002361 T_a \quad (4-6)$$

Where λ is the latent heat of vaporization [J kg^{-1}] and T_a is the temperature [$^{\circ}\text{C}$]. ET was then computed as:

$$ET = \left(\frac{\lambda ET}{\lambda} \right) \quad (4-7)$$

The total ET is the total evapotranspiration [mm s^{-1}]. To get the total ET flux over 30 minute interval the ET was multiplied by 1800s

5. RESULTS AND DISCUSSION

5.1. Comparison of Priestley – Taylor (PT) Model and Measured Evapotranspiration

Priestley – Taylor model ET is the evapotranspiration from moist environment. In the comparison of PT model with measured ET relatively wet environmental conditions were considered. The selected months for relatively wet conditions were March and April. The PT model usually is only used for wet environment.

The results of ET measured in Spain and estimated using the PT for the wet period is shown in the Figure 5-1. The mean daily ET measured in March was 1.6 mm/day while the PT model estimated the potential ET at 1.9 mm/day and their standard deviation was 0.4 mm/day and 0.43 mm/day, respectively. Consequently the daily mean ET difference between PT model and measured ET in March was approximately 0.4 mm/day. According to the basic concept of Aridity ET estimation, most of this difference (PT model minus measured ET) belongs to advection of wind effects. In this March, also the trend was examined. The trend of the PT estimations was similar to measured ET, indicating a good correlation (0.7).

These findings correspond well to the finds of Morton (1978, 1983). He applied the Bouchet's (1963) complementary relationship (CR) and found that the actual ET for the wet months is about the same as the potential ET (by measured data and Penman model). The PT model and AA models predict the evaporation rate well when the radiation was the primary mechanism forcing of the evaporation (Parlange & Katul, 1992).

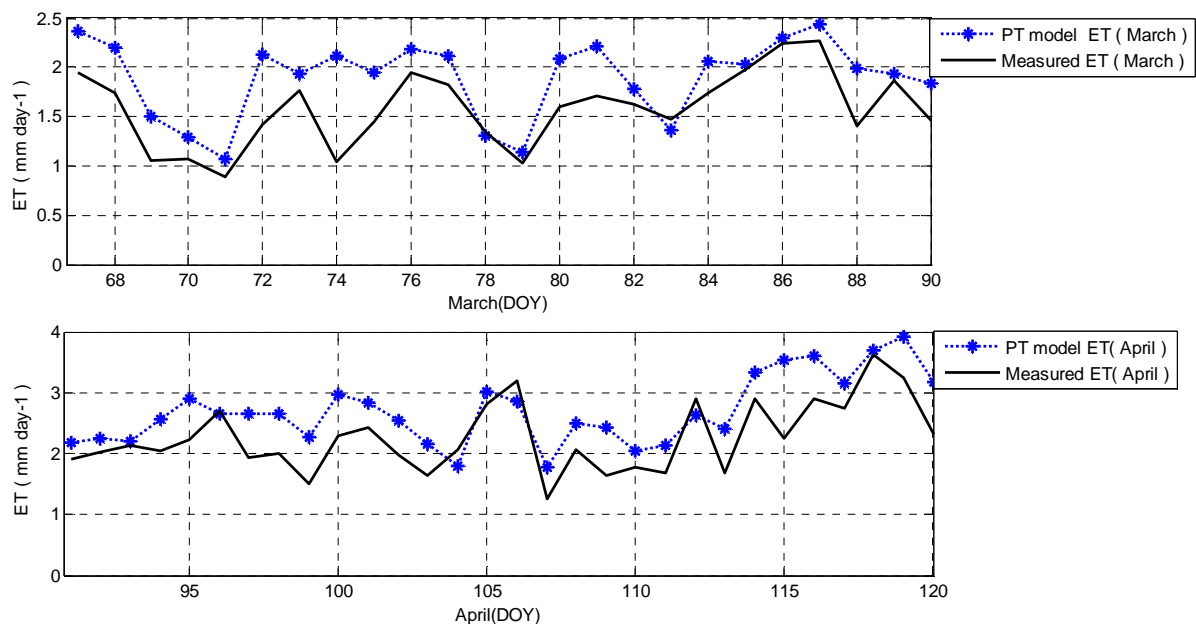


Figure 5-1 : Comparison of average daily PT model with measured ET for the month March and April

5.2. AA Model Validation for Standard Wind Function

5.2.1. AA Model Validation for Standard Wind Function in Wet Conditions

Figure 5-2 and Figure 5-3 shows a comparison of measured ET and modelled ET by using the standard wind function. In the wet period, the mean air temperature was 7.5 °C and the mean RH was 72 %. Table 5-1 shows that when rainfall occurs and relative humidity increases, then the available energy decreases, because rainfall occurs during clouded conditions with low incoming solar radiation and the total number of rainy days and non rainy days. The percentage of rainy and non rainy days was 70 and 29, respectively. In April the total evaporation of AA standard wet was 65.3 mm and of measured ET was 67.9 mm which was twice as large as March ET. The result was pretty good (RMSE = 0.55 mm/day) which was approximated as good as the calibrated wind function presented later. Moreover, the standard wind function was derived based on the wet environment. (Figure 5-2 a & c)

Table 5-1: Rainfall, relative humidity and net radiation for some example days. The data show that net radiation is negatively correlated with rainfall and relative humidity.

DOY	Rainfall (mm/day)	Relative humidity (%)	Net radiation (MJ m ⁻² day ⁻¹)
77	0.1	64	21
78	1.5	75	14.6
79	4	80	8.8
83	5.5	77	12
Total days	Number of rainy days	Number of non rainy days	Percentage of rainy days (%)
70	49	21	70

Table 5-2 : shows the statistics of the results for all the daily analyses

AA model	RMSE (mm/day)	No. of regression analysis days(n)
Standard wet	0.55	71
Standard dry	0.95	45
Measured wet	0.53	71
Measured dry	1.5	45
Calibrated wet	0.4	70
Calibrated dry	0.68	45

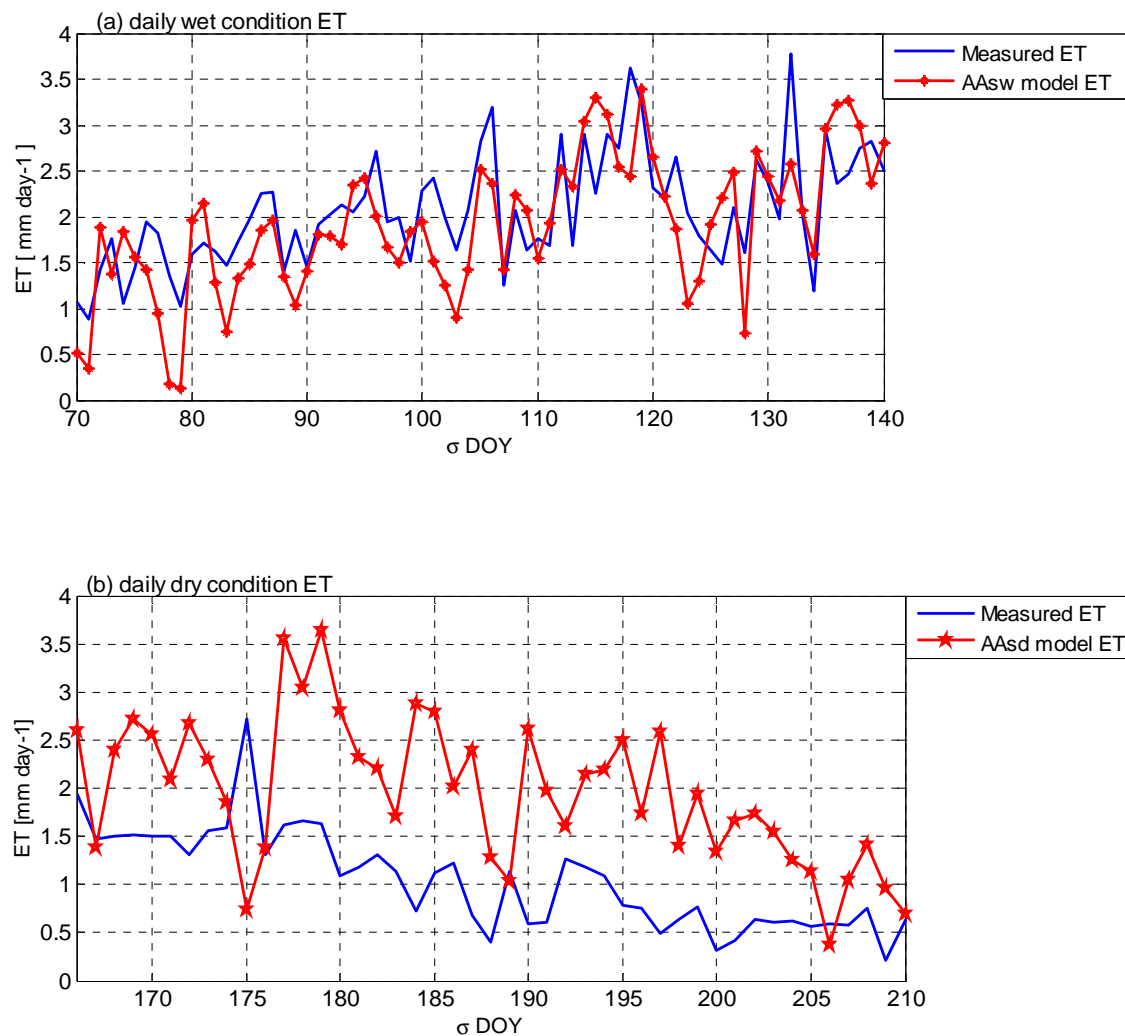
5.2.2. AA Model Validation for Standard Wind Function in Dry Condition

The comparison of AA model for standard wind function in dry condition versus measured ET is presented in Figure 5-2 b & d. The figure shows that the standard model overestimated. This is because of the dryness of the environment. The daily mean air temperature and RH are 23 °C and 46 %, respectively. This shows that the less moisture availability causes to the standard wind function to overestimates in dry condition.

The overestimation of ET increases with increasing dryness of the air. For example, by mid of May to mid of June the monthly measured ET and standard model was 49 mm and 72mm respectively, consequently the difference was 23 mm. hence by mid of May to mid of June, the AA standard overestimates the monthly ET by approximately 46 % and by mid of June to mid of August more than 100 %. In Table 5-2 the linear regression analysis of observation days (n = 45) shows that the RMSE was 0.95 mm/day which also increased in comparison to the preceding months (March and April). Thus the model capacity to dry spells is low when using the standard wind function. As a result of dryness, the Figure 5-2 b & d showed that the increase difference clearly between standard AA model and measured ET.

5.2.3. AA Model Validation for Standard Wind Function under Complementary Relationship

Figure 5-3 Shows that the complementary relation (CR) between the actual and potential ET. The CR was the basic principle to evaluate the AA model result with respect to the given relation mentioned in section 2.6. The moisture index(x – axis) expected to have a maximum of one, and the normalized ET(y – axis) to have a minimum of zero and a maximum of two. Under wetted conditions, it is influenced by the available energy and stayed at the standardized constant normalized line ET is equal to one. Deviation over or under from normalized ET line of one is a matter of wind function effect that is moisture deficit. Under available of moisture both the standardized actual ET and potential ET approach to one while less moisture exists, the normalized ET_a and ET_p approximately zero and two, respectively. The Figure 5-3 shows that the trend was within standard CR relation, but as the dryness was increasing (when moisture index approaches to zero), the trend shows more scatter. This happened for AA standard dry condition (see Figure 5-2 b and d) and the RMSE is high (0.95 mm/day). As a result of dryness, the CR scatters and moisture index was decreasing (see Figure 5-3). Generally the result shows the model with the standard wind function performs better during wet conditions than dry conditions.



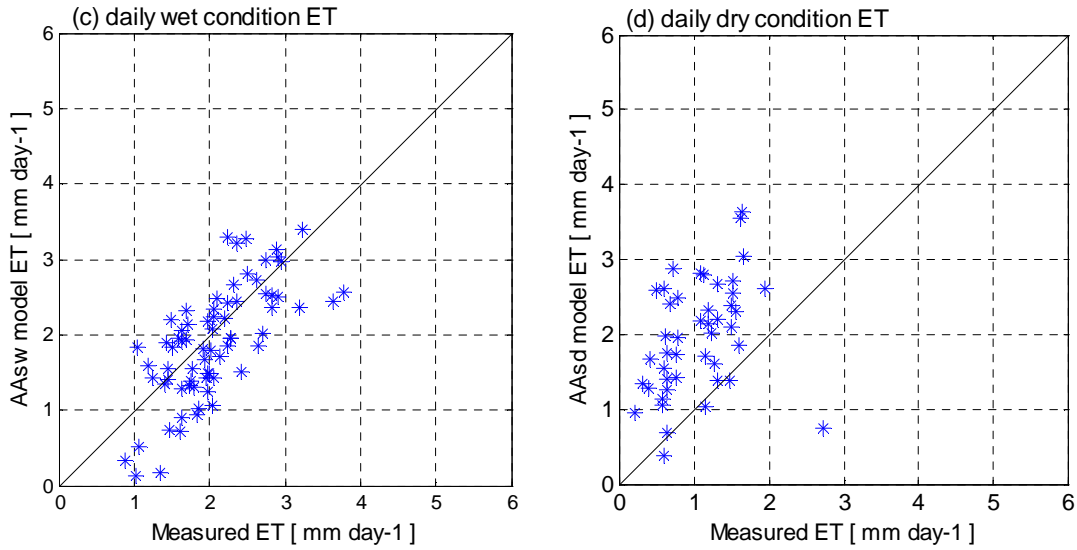


Figure 5-2 : AA model validation for standard wind function

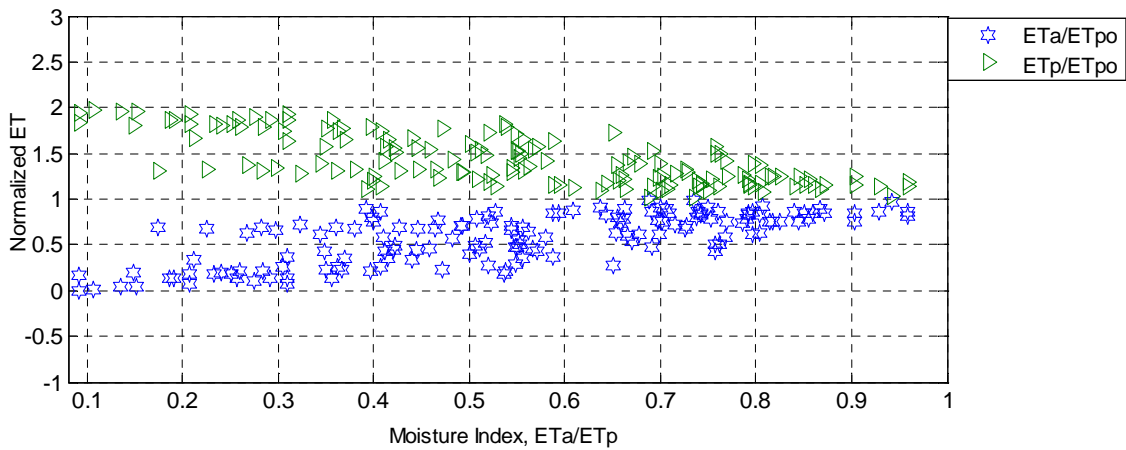


Figure 5-3 : AA model validation for standard wind function under complementary relationship between normalized actual ET and normalized potential ET

5.3. AA Model Validation for Measured Wind Function

5.3.1. AA Model Validation for Measured Wind Function in Wet Conditions

The AA model for measured wind function in wet condition presented in Figure 5-4 a & c. The daily average ET difference between AA measured (2.4 mm/day) model and measured ET (approximately 2 mm/day) was approximately 0.4 mm/day. In Table 5-2 the linear regression analysis of observation (n = 71) shows that the RMSE was 0.53 mm/day. In Table 5-3 the mean in dry (3.6 mm/day) estimated is higher than the wet (2.4 mm/day) condition, but in the measured the ET increases with wetness. The correlation was approximately 0.7. The result is similar with standard wind function of wet. Likewise standard, the measured wind function was pretty good when the relative humidity increases, the air temperature decreases and the rainfall exist under wet than dry condition.

Table 5-3 : Statistical result of daily measured AA ET in mm/day

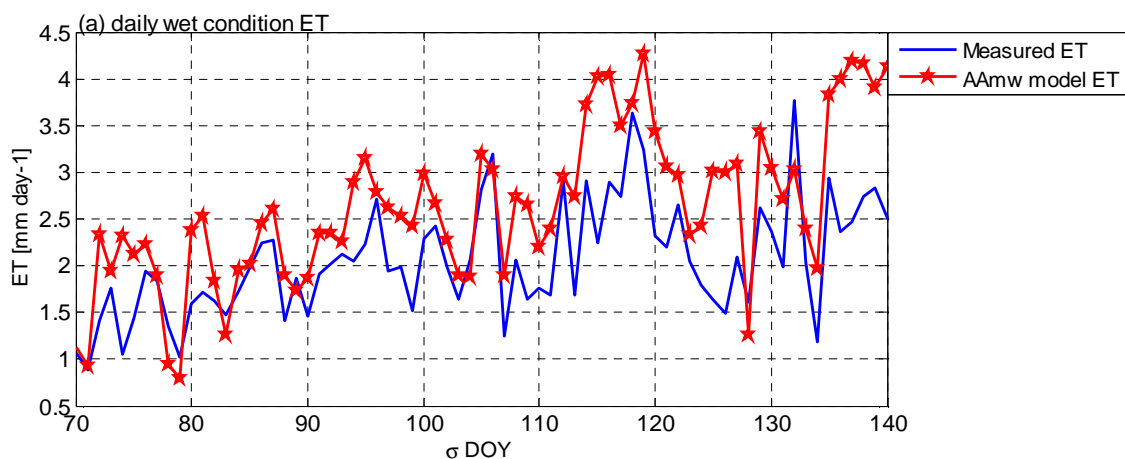
	Mean(mm/day)	Standard dev. (mm /day)	RMSE(mm/ day)	Correlation
Measured AA dry	3.6	0.6	1.5	-
Measured AA wet	2.4	0.8	0.53	0.73

5.3.2. AA Model Validation for Measured Wind Function in Dry condition

In the contrary to wet condition, the ability to apply the measured wind function into AA model for dry condition was less successful (Figure 5-4 b & d). Particularly in comparison to either standard or calibrated wind function. For example, in dry condition, the peak AA measured wind function estimated value was higher than either in standard or calibrated AA model. The largest RMSE of all three wind function was evaluated in the measured dry AA (1.5 mm/day). The only option to calibrate this model is Priestley – Taylor coefficient but even changing this coefficient to the limit of a realistic range is insufficient to fit measured ET. For example, the modelled ET (with measured wind function) was approximately two times higher than the measured ET. Reasons could be 1) that the PT coefficient changes during the dry season 2) model capacity for dry condition are questionable when relating the wind function by wind speed and friction velocity only. Similar to the standard wind function, the measured wind function overestimates ET during the dry period when the relative humidity decreases, air temperature increases and no rainfall exist (see Figure 5-4 b & d).

5.3.3. AA Model Validation for Measured Wind function under Complementary relationship

Considering the complementary relationship of standardized ET, no clear trend was observed (Figure 5-5). As the moisture index decreases from 0.5 (x – axis), the trend did not follow the proposed Bouchet's exponential relationship between the normalized ET and normalized actual ET. The CR trend in dry condition was scattered and the higher discrepancy result shown in Figure 5-4 b & d.



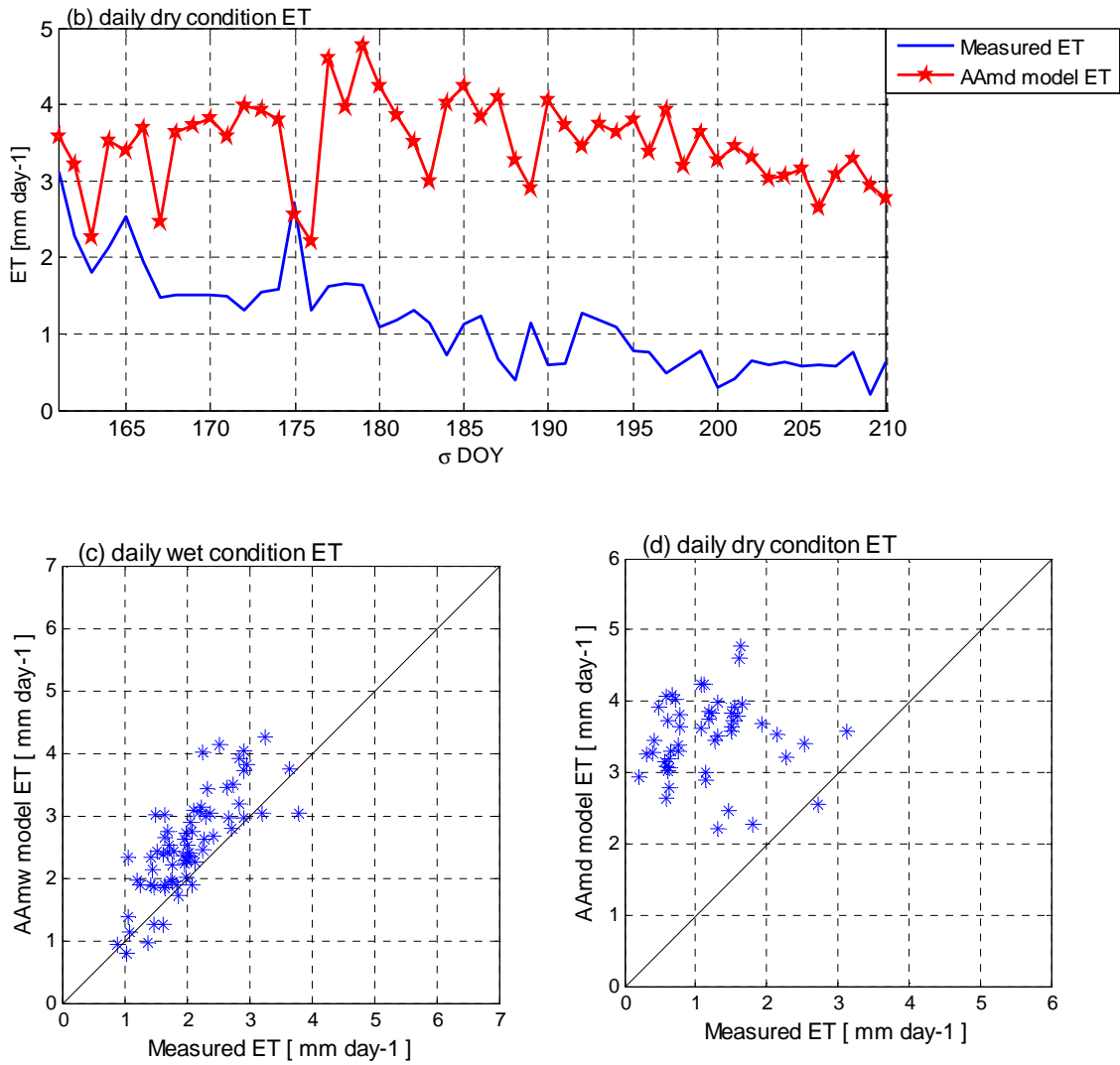


Figure 5-4 : AA model validation for measured wind function

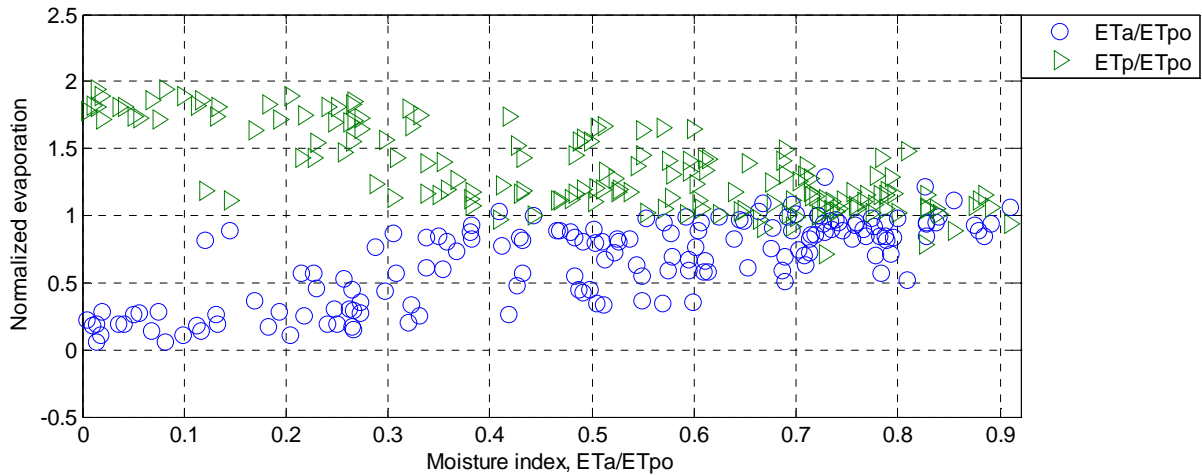


Figure 5-5 : AA model validation for measured wind function under complementary relationship between normalized actual ET and normalized potential ET

5.4. AA Model Validation for Calibrated Wind Function

5.4.1. AA Model Validation for Calibrated Wind Function in Wet Conditions

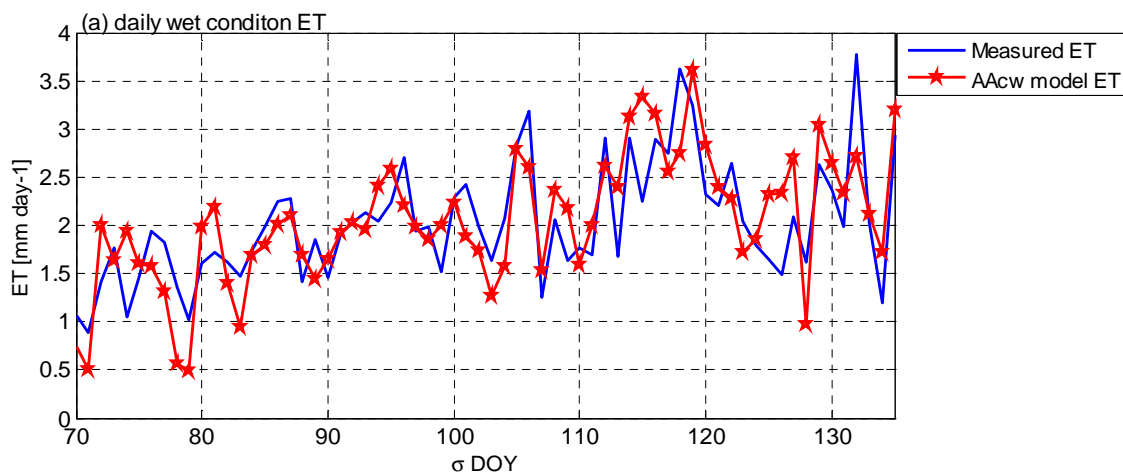
The result presented in Figure 5-6 a & d and In Table 5-2. The linear regression analysis of observation days ($n = 70$) provided that the RMSE was 0.4 mm/day. The daily mean ET difference between calibrated and measured ET was less than 0.4 mm day⁻¹. When compared with the standard (RMSE = 0.55) and measured (RMSE= 0.53) wind function, the calibrated was better approximated to the measured eddy tower ET. The Figure 5-6 shows that the coefficient of determination is approximately 0.7 and the regression line is close to one to one. The result shows likewise standard and measured it was in a good agreement with measured ET.

5.4.2. AA Model Validation for Calibrated Wind Function in Dry condition

The result for the optimized AA model for dry conditions is presented in Figure 5-6 b & d. The best fit coefficient and constants for empirical wind function occurred where the daily mean actual ET less than 2 mm/day. The calibrated was better than the preceding overestimated two wind functions (i.e. Standard and measured under dry). The statics obtained from the regression are presented in Table 5-2. In the dry environmental condition, the RMSE of standard (0.95 mm/day) and the measured (1.5 mm/day) wind function shows that higher than calibrated (0.68 mm/day) (see Figure 5-2 and Figure 5-4 b & d). Ali et al.,(1987) mentioned a number of causes for the discrepancy possibility of AA model. Under dry condition for example the incorrect choice for the value of Priestley - Taylor coefficients and deficiencies of the model too.

5.4.3. AA Model Validation for Calibrated Wind function under Complementary relationship

The CR relation was evaluated for the calibrated AA model and presented in Figure 5-7. The analysis shows a good agreement for both dry and wet conditions. The CR relationship is again evaluated through considering the moisture availability response to Normalized ET which is standardized of dividing ET_a and ET_p by ET_{po} . According to the CR relation of Figure 5-7, increasing wetness moves the ET_a and ET_p pair to the right towards convergence of their respective curves, while decreasing the Sardon wetness moves the ET_a and ET_p pair divergently to the left. Increasing ET_p case is a change in more radiation. In the decrease of wetness and increase of net radiation – shifts ET_a to downward. This result shows the principle interpretation of the relationship in accordance with CR, the decrease of ET_a or increase of ET_p is a similar way.



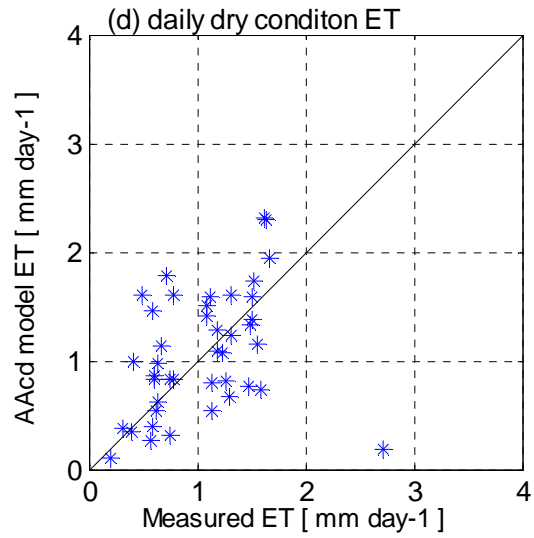
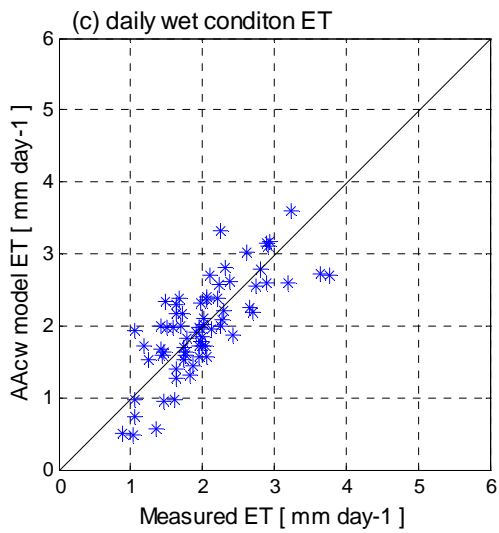
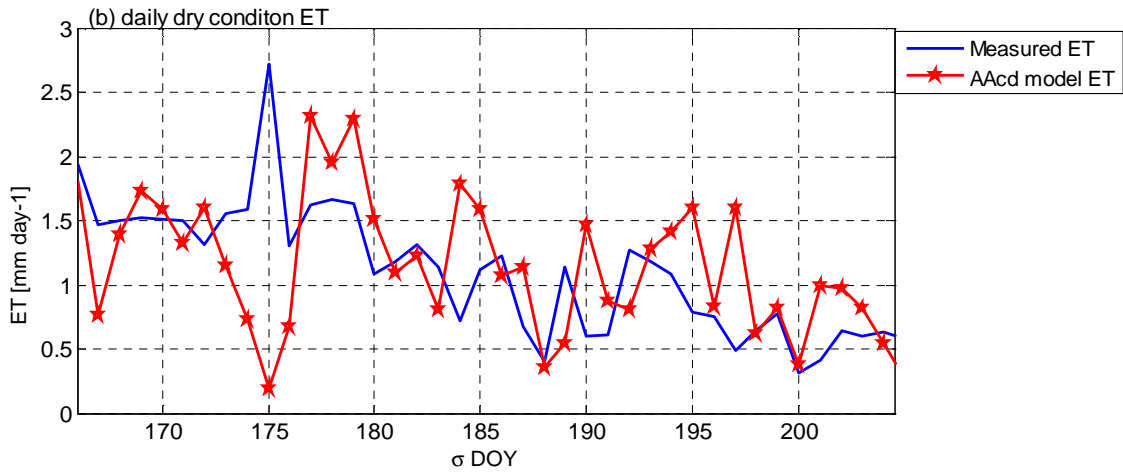


Figure 5-6 : AA model validation for a calibrated wind function

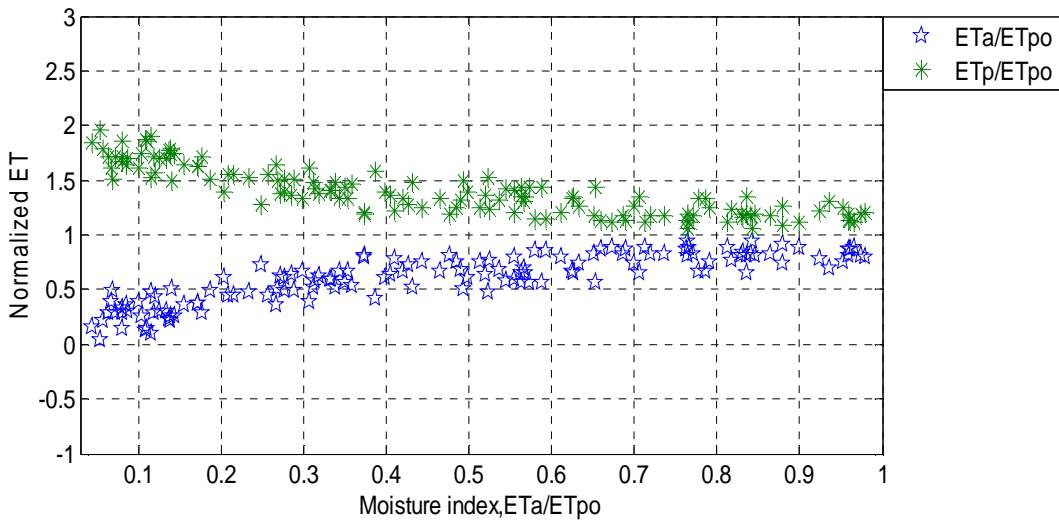


Figure 5-7 : AA model validation for daily calibrated wind function in terms of complementary relationship between actual ET and potential ET

5.5. Half hourly AA Model Validation

5.5.1. Half Hourly AA Model Validation for Standard Wind Function

Figure 5-8 shows the half hourly AA model ET estimates using the standard wind function for both wet and dry conditions.

- In the wet condition, the available energy (net radiation minus ground heat flux) varies from 0 to 500 W m^{-2} . The estimated latent heat by the standard model was 0 to 420 W m^{-2} and by measured ET which had a maximum of 300 W m^{-2} .
- In dry condition, the standard model the maximum λET estimates is 580 W m^{-2} while the maximum measured ET is 150 W m^{-2} .

This shows the existence of different responses for different weather conditions for measured ET, which are not well captures by the standard model. As available energy is higher in dry condition, the standard model estimates are higher but the actual ET considers the moisture availability hence estimates decreases.

5.5.2. Half Hourly AA Model Validation for Standard Wind Function In terms of Complementary Relationship

Figure 5-9 shows half hourly model validation in terms of the complementary relationship. There is no clear compensation between the standardized actual ET and standardized potential ET. when the normalized ET under or over from the line equals to one, both standardized actual ET and standardized potential ET scatter towards to zero and two, respectively. The compensation figure shows similar scatter result under either wet or dry condition.

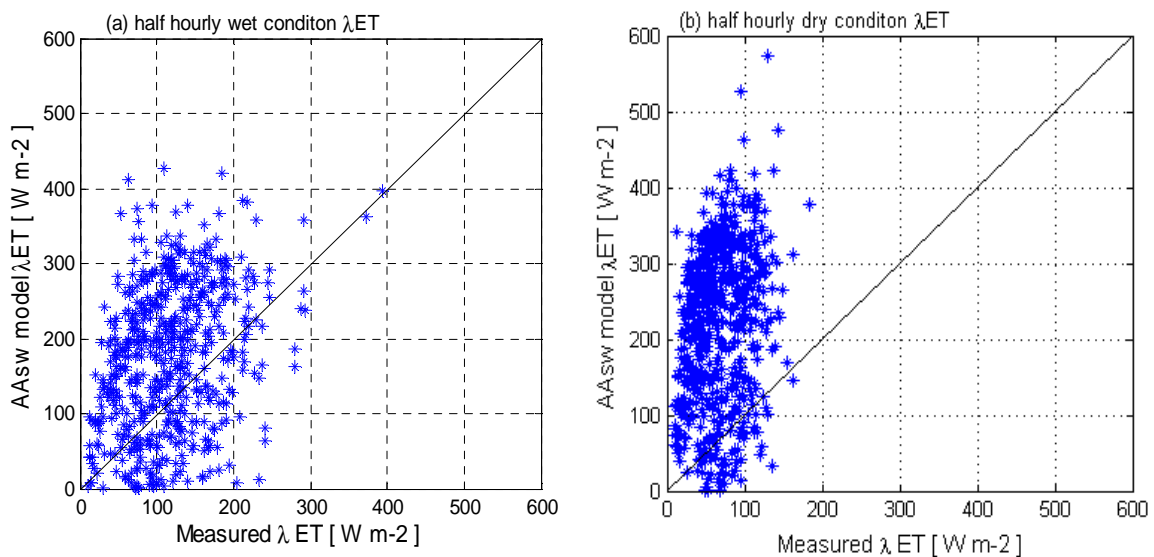


Figure 5-8 : AA model validation for half hourly standard wind function

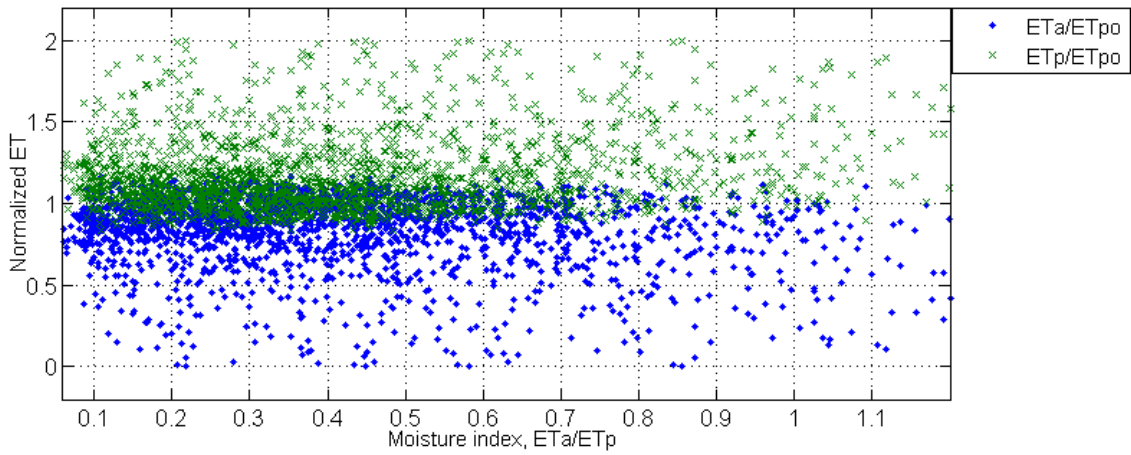


Figure 5-9 : AA model validation for half hourly standard wind function

5.5.3. Half Hourly AA Model Validation for Measured Wind Function In terms of Complementary Relationship

Figure 5-10 shows the half hourly measured wind function ET estimates. The result resembles the same as Standard AA model but in the wet condition has more scatter towards to overestimation. Similar to standard AA model, the measured wind function overestimates latent heat.

Table 5-4 shows the statistical result of the half hourly analysis with low correlation and high RMSE observed in wet condition is 0.3 and 105 W m⁻² and in dry condition 0.2 and 120 W m⁻², respectively. The standard deviation (SD) from the mean of AA model in wet was 167 Wm⁻² and in dry 226 W m⁻². Consequently the higher value of SD was in case of wet (50 W m⁻²) than dry (35 W m⁻²). The SD increases from dry to wet in case of measured AA model and decreased in case of measured ET.

Table 5-4 : Statistical result of half hourly measured AA and eddy tower measured ET in W m⁻²

	Mean(Wm ⁻²)	Standard deviation(W m ⁻²)	RMSE (W m ⁻²)	Correlation
Measured AA dry	226	113	120	0.2
Measured AA wet	167	90	105	0.3
Measured ET dry	86	35	–	–
Measured ET wet	106	50	–	–

5.5.4. Half Hourly AA Model Validation for Measured Wind Function In terms of Complementary Relationship

The Figure 5-10 complementary relationship result shows no clear compensation between the standardized actual ET and potential ET as it was presented for the half hourly standard wind function. Both scatter above or below from the normalized ET equals one. The complementary relationship is a good indication to the accuracy of model result. As we had seen in the previous section either for daily or half hourly when the discrepancy increases the compensation trend between standardized actual ET and potential ET scatters more.

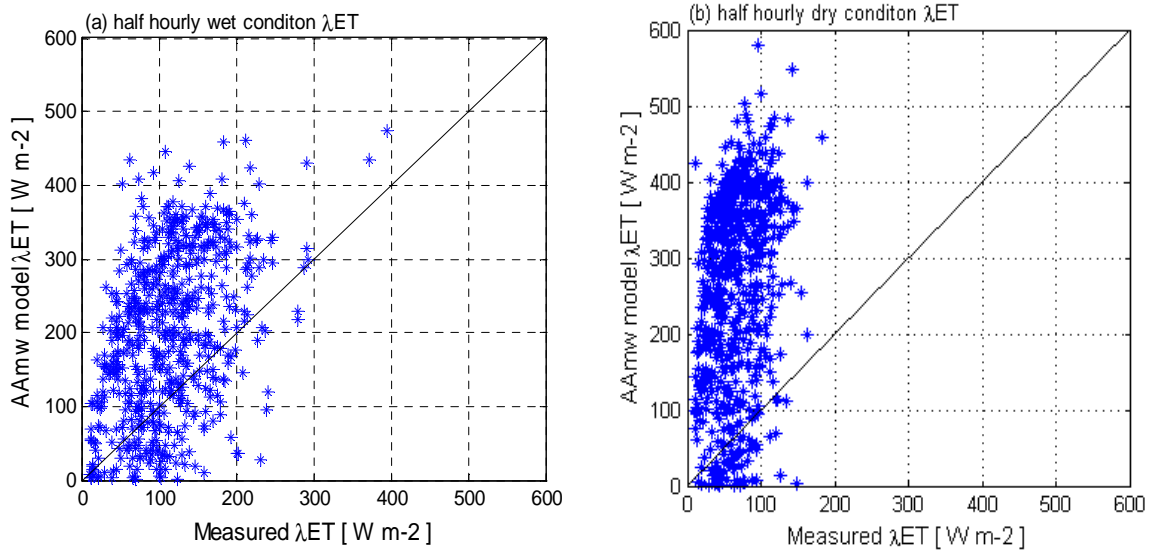


Figure 5-10 : AA model validation for half hourly measured wind function

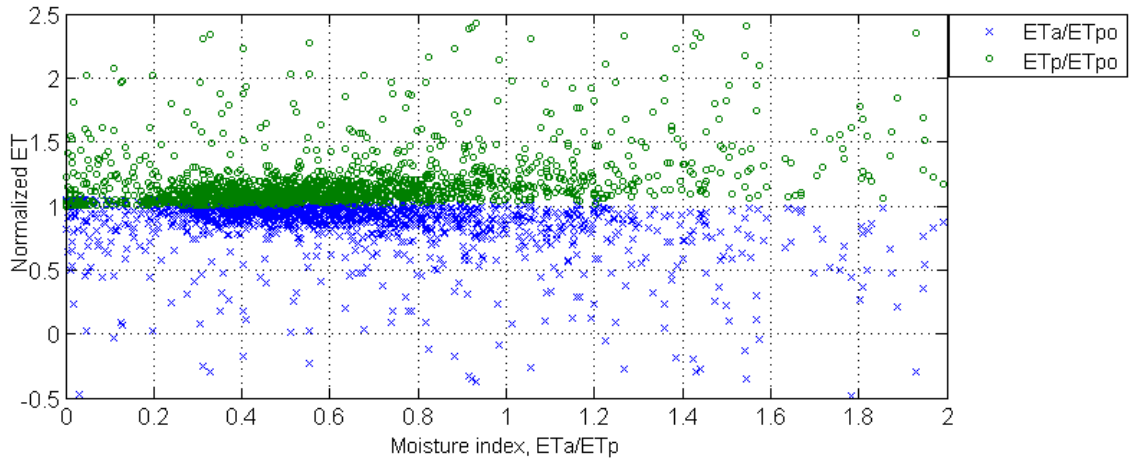


Figure 5-11 : AA model validation for half hourly measured wind function in terms of complementary relationship between actual and potential ET

6. CONCLUSIONS AND OUTLOOK

6.1. Conclusions

We have investigated actual evapotranspiration by the Advection Aridity method over the Sardon area. Using ground based measurements the effects of wet and dry conditions and temporal resolution of the data have been investigated. The investigation was performed successfully, as each of the sub objectives was concluded.

To investigate the proper wind function to run the Advection Aridity model

- The AA model run with three wind function, 1) standard, 2) measured which was proposed in terms of friction velocity, wind speed and density of the air, and 3) empirically calibrated wind function. The AA model estimate accuracy of those three wind function depends on the atmospheric weather condition (Wet or dry). The better estimates of all three wind function are the calibrated one.
- With respect to ET measuring instrument access, for Africa, the standard is applicable especially in the wet condition when similar weather exists to Sardon, Spain. But for dry weather, at least it needs to be calibrated. The less applicable wind function is the measured which requires the friction velocity measuring instrument that is expensive to afford into Africa.

To evaluate the accuracy of the model during relatively wet and dry condition

- In wet condition the standard, measured and calibrated shows that the RMSE 0.55, 0.53 and 0.4 mm/day, respectively. The results approximated to the actual measurement. Moreover, the model result supported by the trend of complementary relationship.
- In a dry condition the standard and measured shows that the RMSE (root mean square error) were 0.95 mm/day and 1.5 mm/day. By mid of the May to mid of June, the standard estimates 46% higher than the eddy tower measured ET and the measured wind function estimates two times higher than the actual eddy tower ET. Under dry condition, the validation of both standard and measured AA model result shows that was scatter and overestimated. The calibrated AA model was better than the preceding overestimated standard and measured wind function, but less compared to wet condition. The RMSE of calibrated was 0.68 mm/day and the trend was evaluated in a good agreement with the complementary relationship.

To evaluate effect of the temporal resolution on the accuracy of the model

- The daily AA model shows a lower RMSE (as it was mentioned before) and a clear trend of complementary relation than half hourly AA model. The statistical result of the half hourly analysis with low correlation and high RMSE observed in wet condition is 0.3 and 105 $W m^{-2}$ and in dry condition 0.2 and 120 $W m^{-2}$, respectively. The increased discrepancy made no clear complementary relationship trend between the standardized actual ET and Potential ET and shows scatter. Thus the AA model have a predict power for daily than half hourly.

6.2. Outlook

What should be done in the future!

- My interest for the future is research on to integrate the advection aridity model with Satellite products.
- As Brutsaert (2005) mentioned no general accepted wind function, the investigation on wind function equation is recommended.

LIST OF REFERENCES

- Ali, M. F., & Mawdsley, J. A. (1987). Comparison of two recent models for estimating actual evapotranspiration using only regularly recorded data. *Journal of Hydrology*, 93(3-4), 257-276.
- Allen, R. G., Pereira, L. S., Raes, D., & Smith, M. (1998). *Crop evapotranspiration: guidelines for computing crop water requirements*. FAO irrigation and drainage paper; 56. FAO, Rome, 300 pp.
- Bastiaanssen, W. G. M., Menenti, M., Feddes, R. A., & Holtslag, A. A. M. (1998). A remote sensing surface energy balance algorithm for land (SEBAL). *Journal of Hydrology*, 212-213, 198-212.
- Bouchet, R. J. (1963). Evapotranspiration réelle, évapotranspiration potentielle, et production agricole. *Ann. Agron.*, 14, 743-824.
- Bouchet, R. J. (1963). Evapotranspiration réelle, évapotranspiration potentielle, et production agricole. *Ann. Agron.*, 14, 743-824.
- Brusaert, W. (2005). *Hydrology: An Introduction*, Cambridge University Press, Cambridge, 605 pp.
- Brutsaert, W. (1982). *Evaporation into the atmosphere: theory, history, and applications*. Reidel Publishing, Dordrecht etc., 299 pp.
- Brutsaert, W., & Stricker, H. (1979). An advection - aridity approach to estimate actual regional evapotranspiration. *Water Resour. Res.*, 15, 443-450.
- Campbell scientific, 1994. CSA 3 3-D Sonic Anemometers. <http://www.campbellsci.com/documents/product-brochures/bcsat3.pdf>. Oct 26
- Gash, J. H. C., & Shuttleworth, J. E. (2007). *Evaporation. Benchmark paper in hydrology*; International Association of Hydrological Sciences (IAHS), Wallingford, 131 pp.
- Glenn, E. P., Huete, A. R., Nagler, P. L., Hirschboeck, K. K., & Brown, P. (2007). Integrating remote sensing and ground methods to estimate evapotranspiration. *Critical Reviews in Plant Sciences*, 26(3), 139-168.
- Granger, R., & Gray, D. (1990). Examination of Morton's CRAE model for estimating daily evaporation from field-sized areas. *J Hydrol* 120: 309-325.
- Haque, A. (2003). Estimating actual areal evapotranspiration from potential evapotranspiration using physical models based on complementary relationships and meteorological data. *Bull Eng Geol Env* (2003) 57-63.
- Hobbins, M. T., Ramirez, J. A., & Brown, T. C. (2001b). The complementary relationship in estimation of regional evapotranspiration: an enhanced advection-aridity model. *Water Resour. Res.*, 37, 1389-1403.
- Kalma, J. D., McVicar, T. R., & McCabe, M. F. (2008). Estimating Land Surface Evaporation: A Review of Methods Using Remotely Sensed Surface Temperature Data. *Surveys in Geophysics*, 29(4-5), 421-469.
- Kipp, Z. (2002). *CNR 1 Net radiometer Instruction Manual*, Delft, the Netherlands, pp.46.
- Kustas, W. P., & Norman, J. M. (2000). A Two-Source Energy Balance Approach Using Directional Radiometric Temperature Observations for Sparse Canopy Covered Surfaces. *Agron J*, 92(5), 847-854.
- Lemur, R., & Zhang, L. (1990). Evaluation of three evapotranspiration models in terms of their applicability for an arid region. *Journal of Hydrology* 114: 395-411
- Liu, J., & Kotoda, K. (1998). Estimation of regional evapotranspiration from arid and semi-arid surfaces. *Journal of the American Water Resources Association* 34(1): 27-40.
- Lubczynski, M. W., & Gurwin, J. (2005). Integration of various data sources for transient groundwater modelling with spatio-temporally variable fluxes-Sardon study case, Spain. *Journal of Hydrology*, 306(1-4): 71-96.
- Monteith, J. L. (1965). Evaporation and the environment. *Sym. Soc. Exp. Biol.* 19, 245-269.
- Morton, F. I. (1976). Climatological estimates of evapotranspiration. *J Hydraul Div Proc ASCE* 102(HY3): 275-291.
- Morton, F. I. (1978). Estimating evapotranspiration from potential evaporation: practicality of an iconoclastic approach. *J Hydrol* 38: 1-32.
- Morton, F. I. (1983). Operational estimates of areal evapotranspiration and their significance to the science and practice of hydrology. *J Hydrol* 66: 1-76.
- Ontiveros Enriquez, R. (2009). *Tree transpiration : a spatio - temporal approach in water limited environments, Sardon study case*. Enschede, ITC, 2009. 65 p.
- Parlange, M. B., & Katul, G. G. (1992). An advection-aridity model. *Water Resour. Res.*, 28: 127-132.

- Penman, H. L. (1948). Natural evaporation from open water, bare soil, and grass., Proc. R. Soc. London, A 193, 120-146.
- Penman, H. L. (1956). Evaporation:an introductory survey. Netherl.J.Agric.Sci., 4, 9-29 pp.
- Priestly , C., & Taylor, R. (1972). On the assessment of surface heat flux and evaporation using large - scale parameters. Monthly Weath Review, 100: 81-92.
- Ruwan Rajapakse, R. R. G. (2009). Numerical groundwater flow and solute transport modelling:a case study of Sardon catchment in Spain. Enschede, ITC, 2009. 92 p.
- Rwasoka, D. T. (2010). Evapotranspiration in water limited environments : up - scaling from crown canopy to the eddy flux foot print.Enschede, ITC, 2010. 79 p.
- Slatyer, R. O., & Mollry, I. C. (1961). Practical Microclimatology. Melbourne, Ausralia: CSIRO.
- Su, Z. (2002). The Surface Energy Balance System (SEBS) for estimation of turbulent heat fluxes. Hydrology and Earth System Sciences, 6(1), 85-99.
- Thom, A. S. (1975). Momentum, mass and heat exchange. In: Monteith, J.L., (Ed), Vegetation and the Atmosphere, Volume 1, Principles, Academic Press, London.
- Thorntwaite, C. W. (1948). An approach toward a rational classification of climate. Geograph. Rev.,38, 55-94.
- Twine, T. E., Kustas, W. P., Norman, J. M., Cook, D. R., Houser, P. R., Meyers, T. P. et al. (2000). Correcting eddy-covariance flux underestimates over grassland. Agricultural and Forest Meteorology, 103(3): 279 - 300.
- van der Tol, C., Gash, J. H. C., Grant, S. J., McNeil, D. D., & Robinson, M. (2003). Average wet canopy evaporation for a Sitka spruce forest derived using the eddy correlation-energy balance technique. Journal of Hydrology, 276(1-4), 12-19.
- WMO. (1994). World Meteorological Organization, 1994: Guide to Hydrological Practices. Fifth edition, WMO No.168, Geneva.
- Xu, C. Y., & Singh, V. P. (2005). Evaluation of three complementary relationship evapotranspiration models by water balance approach to estimate actual regional evapotranspiration in different climatic regions. Journal of Hydrology, 308(1-4), 105-121.
- Xu, X., & Li, J. (2003). A distribute approach for estimatiing catchment evapotranspiration: comparison of the combination equation and the complementary relationship appraoches. Hydrol. process.17. 1509 - 523.
- Zhang, Y., Liu, C., Yu, Q., Shen, Y., Kendy, E., Kondoh, A. et al. (2004). Energy fluxes and Priestley–Taylor parameter over winter wheat and maize in the North China Plain. Hydrological Processes 18: 2235–2246.

Appendix

Appendix A Matlab code conversion half hourly into daily

```

D:\field_data\Sardon_Updated\Matlab\2010\makedaily010.m
File Edit Text Go Cell Tools Debug Desktop Window Help
% calculate the daily values with the function 'makedaily.m'
% 1. RADIATION[watt per meter ^2]
% 1.1
[Rsi_mean,-] = makedaily(t,Rsi,0,[0,1137],2);
Rsi_min = makedaily(t,Rsi,2,[-5,5],10);
Rsi_max = makedaily(t,Rsi,3,[0,1200],10);
% 1.2
[Rso_mean,-] = makedaily(t,Rso,0,[0,238],2);
Rso_sum = makedaily(t,Rso,1,[0,20000],10);
Rso_min = makedaily(t,Rso,2,[0,1000],10);
Rso_max = makedaily(t,Rso,3,[0,1000],10);
% 1.3
[Rli_mean,-] = makedaily(t,Rli,0,[194,426],2);
Rli_sum = makedaily(t,Rli,1,[0,20000],10);
Rli_min = makedaily(t,Rli,2,[100,400],10);
Rli_max = makedaily(t,Rli,3,[100,500],10);
% 1.4
[Rlo_mean,-] = makedaily(t,Rlo,0,[285,634],2);
Rlo_sum = makedaily(t,Rlo,1,[0,20000],10);
Rlo_min = makedaily(t,Rlo,2,[0,1000],10);
Rlo_max = makedaily(t,Rlo,3,[0,1000],10);
% 1.5
Rn_mean = Rsi_mean + Rli_mean - Rso_mean - Rlo_mean;
% 2. METEOROLOGICAL PARAMETER
% 2.1 Relative Humidity
[Rh_mean,Rh_q,-] = makedaily(t,Rh,0,[0,100],2);
Rh_min = makedaily(t,Rh,2,[0,100],2);
Rh_max = makedaily(t,Rh,3,[0,100],2);
% 2.2 Rainfall
[R_sum,R_q,-] = makedaily(t,Rain,1,[0,1400],1);
% 2.3 wind speed
[u_mean,u_q,-] = makedaily(t,u,0,[0,7],2);
u_min = makedaily(t,u,2,[0,7],2);
u_max = makedaily(t,u,3,[0,7],2);

D:\field_data\Sardon_Updated\Matlab\2010\makedaily.m
File Edit Text Go Cell Tools Debug Desktop Window Help
function [d,quality,days] = MakeDaily(time,data,m,OC,Nmin)
%function d=MakeDaily(time,data,start,finish,OC,Nmin) converts a matrix of
%data into daily average (m=0) or sum values (m=1), minimum (m=2) or
% maximum (m=3)
%The output: daynumber
%next columns: daily data
%last column:zeros and ones, where 1 means that there were missing
%values during this day.
%optional: give start and finish (integer Julian daynumbers)
%optional: give OC (quality control): two numbers indicating the minimum and maximum value of
% Nmin: the minimum number of data points on a day
start = ceil(min(time));
finish = floor(max(time));
interval = time(2)-time(1);
n2 = size(data,2);
if nargin<5
    Nmin = 1;
end
[d,quality] = deal(NaN*zeros(finish-start+1,n2));
days = (1:finish)';
for i = start:finish
    f=find((time<=i+1) & (time>=i));
    for j=1:length(f)
        if nargin<5
            f=find((time<=i+1) & (time>=i) & data(:,j)<OC(2) & data(:,j)>OC(1));
        end
        z = find(~isnan(data(f,j)));
        if length(z)>Nmin
            switch m
            case 0
                d(i,j) = mean(data(f(z),j));
            case 1
                d(i,j) = sum(data(f(z),j));
            case 2
                d(i,j) = min(data(f(z),j));
            otherwise
                d(i,j) = max(data(f(z),j));
            end
        else
            d(i,j) = NaN;
        end
    end
    quality(i) = length(z);
end
end

```

Appendix B code to determine calibration constants

```

D:\field_data\Sardon_Updated\Matlab\2010\alphaam.m
File Edit Text Go Cell Tools Debug Desktop Window Help
% 180 %
% 181 % subplot(2,1,2)
% 182 ETpe_jun = plot(days_F(djunE), Epe_E(days_F(djunE)));
% 183 legend('Advection Free ET (June)', 'Measured ET (June)');
% 184 xlabel('June (DOY)');
% 185 ylabel('ET in mm day-1');
% 186 title('Comparison of Advection Free ET with Measured');
% 187 set(ETpe_jun,'linewidth',1.5,'markersize',11);
% 188 grid on
% 189 %
% 190 %
% 191 ETpe_july = figure('Position',[1600 320 56200 3]);
% 192 ETpe_july2 = axes('FontSize',14);
% 193 subplot(2,1,1)
% 194 ETpe_july = plot(days(djul), Epe(days(djul)),'r');
% 195 legend('Advection Free ET (July)', 'Measured ET (July)');
% 196 xlabel('July (DOY)');
% 197 ylabel('ET in mm day-1');
% 198 title('Comparison of Advection Free ET with Measured');
% 199 set(ETpe_july,'linewidth',1.5,'markersize',11);
% 200 grid on
% 201 %
% 202 %
% 203 % subplot(2,1,2)
% 204 ETpe_august = plot(days(daug), Epe(days(daug)),'r');
% 205 legend('Advection Free ET (August)', 'Measured ET (August)');
% 206 xlabel('August (DOY)');
% 207 ylabel('ET in mm day-1');
% 208 title('Comparison of Advection Free ET with Measured');
% 209 set(ETpe_august,'linewidth',1.5,'markersize',11);
% 210 grid on
% 211 %
% 212 %
% 213 ETpe_september = plot(days(dsep), Epe(days(dsep)));
% 214 legend('Advection Free ET (September)', 'Measured ET (September)');
% 215 xlabel('September (DOY)');
% 216 ylabel('ET in mm day-1');
% 217 title('Comparison of Advection Free ET with Measured');
% 218 set(ETpe_september,'linewidth',1.5,'markersize',11);
% 219 grid on
% 220 %
% 221 % Stations for Brutsert page 27
% 222 %
% 223 % max((LE_mean_d(dmar))/lambda_d(dmar)),max(Epe(dmar)
% 224 % min((LE_mean_d(dmar))/lambda_d(dmar)),min(Epe(dmar)
% 225 % min((LE_mean_d(dmar))/lambda_d(dmar)),min(Epe(dmar)

D:\field_data\Sardon_Updated\Matlab\2010\alphaam.m
File Edit Text Go Cell Tools Debug Desktop Window Help
% 1 = c1c
% 2
% 3 %load observations
% 4 obs = LE_mean_d(idayyy)/lambda_d(idayyy);
% 5 es_gamma = (esvp_d(idayyy)/(gamma_d(idayyy) + esvp_d(idayyy)));
% 6 q1_d = (Rn_mean_d(idayyy) - Go_mean_d(idayyy))/lambda_d(idayyy);
% 7
% 8 gamma_es = gamma_d(idayyy)/(gamma_d(idayyy) + esvp_d(idayyy));
% 9
% 10 eal = 0.33.*(1.186+ 0.2.*u_mean(idayyy)).*(esvp_d(idayyy) - ea_mean_1(idayyy)).*10;
% 11
% 12 alpa = 110.0013;
% 13
% 14
% 15 [Alpa,Obs] = meshgrid(alpa,obs);
% 16 [-,Es_gamma] = meshgrid(alpa,es_gamma);
% 17 [-,Q1_d] = meshgrid(alpa,q1_d);
% 18 [-,Eal] = meshgrid(alpa,eal);
% 19 [-,Gamma_es] = meshgrid(alpa,gamma_es);
% 20
% 21 Etd1 = (Es_gamma).* Q1_d.*(2.*Alpa - 1) - Eal.*Gamma_es;
% 22 clear Es_gamma Q1_30 Eal Gamma_es
% 23
% 24 rmse = sqrt(nansum((Obs - Etd1).^2,1));
% 25 lmin = min(rmse)==rmse;
% 26 alpa(lmin)
% 27 length(alpa)
% 28
% 29 % find smallest error and correspoding scenario
% 30 plot(alpa,rmse)
% 31
% 32
% 33 c = 1.105
% 34
% 35 i = -(ET30<0 | Obs<0);
% 36 rmse2 = sqrt(mean((Obs(i) - ET30(i)).^2));
% 37 lmin2 = min(rmse2)==rmse2;
% 38 c(lmin2)
% 39 length(c)
% 40 plot(c,rmse2)
% 41
% 42

```

Appendix C code of regression analysis (accuracy assessment by using root mean square error)

```

D:\field_data\Sardon_Updated\Matlab\2010\linreg.m
le Edit Text Go Cell Tools Debug Desktop Window Help
- 1.0 + + 1.1 x
function [p,Sy,N,Sp] = linreg(x,y,intercept)
% [p,Sy,N] = linreg(x,y,intercept)
% LINREG performs linear least square regression
% x : independent, column vector
% y : dependent, column vector
% intercept : 0 forces the function y = p*x through the origin
% default: -> 0 computes the y-intercept p(2) in
% y = p(1)*x + p(2)
% p : regression constants
% Sy : Standard Error of Y-estimated
% N : Number of data points
% Het voordeel van je eigen slimme functie is dat 'ie zelf je NaN-etjes weghaalt,
% dat is iets waar de vernuftige meneer Matlab nog niet opgekomen was.
if nargin == 2
intercept = 1;
end
if intercept > 1
intercept = 1;
end
I = find(~isnan(x) & ~isnan(y));
if size(I,1) > 1+intercept
x = x(I);
y = y(I);
else
N = 0;
if intercept == 0
p = NaN;
Sy = NaN;
Sp = NaN;
else
p = [NaN NaN];
Sy = [NaN NaN];
Sp = [NaN NaN];
end
return;
end
n = size(x,1);
Sx = sum(x);
Sxx = sum(x.^2);
Sxy = sum(x.*y);
Syy = sum(y.^2);
Mx = mean(x);
My = mean(y);
Dx = x - Mx;
Dy = y - My;

```

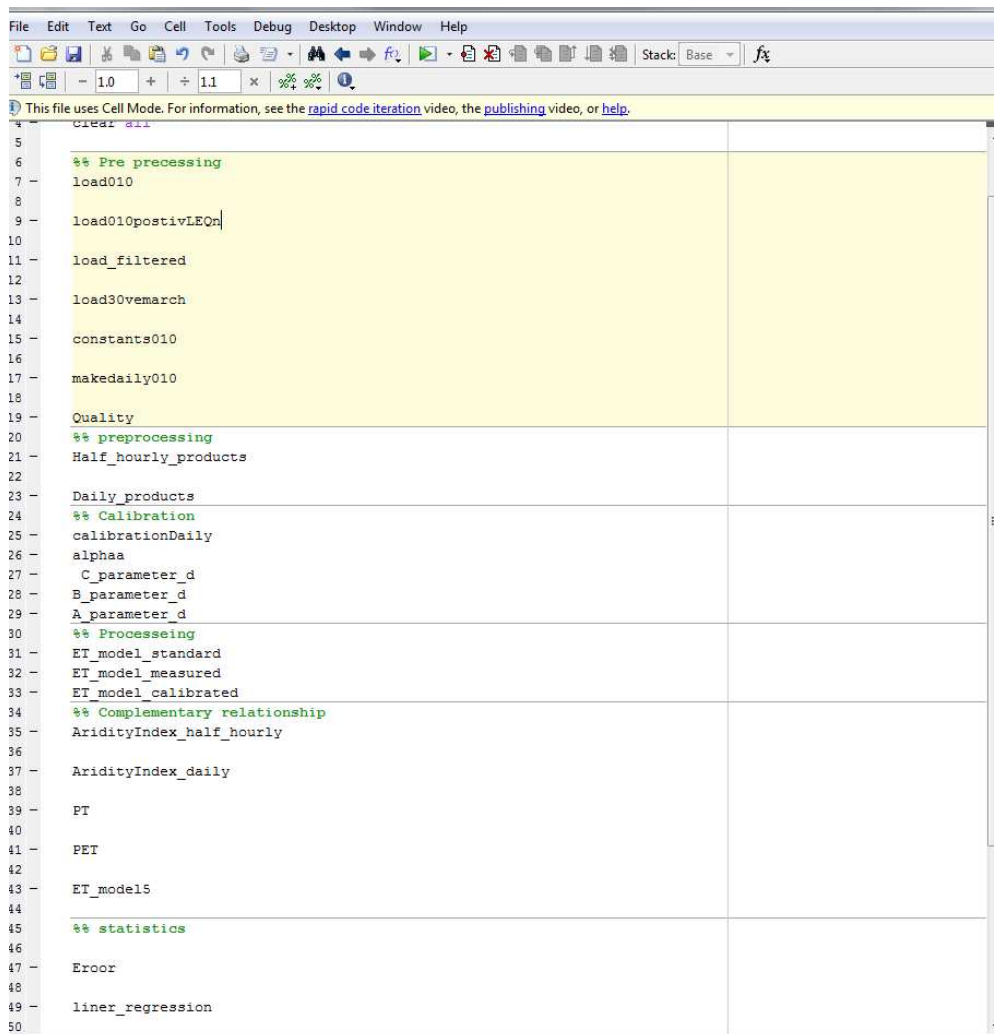
Appendix C Pre-processing products code on Matlab

```

D:\field_data\Sardon_Updated\Matlab\2010\preprocessing.m
le Edit Text Go Cell Tools Debug Desktop Window Help
- 1.0 + + 1.1 x
This file uses Cell Mode. For information, see the rapid code iteration video, the publishing video, or help.
12
13 %% 4. 30 minute (Brutsaert page 47) measured transfer wind function
14
15 %% 4.1 potential evaporation
16
17 Ep30_4 = (esvp_30 ./ (gamma_30 + esvp_30)) .* Onpositive30 + gamma_30 ./ (gamma_30 + esvp_30) ;
18
19 %% 4.2 Actual evapotranspiration
20 Etp30 = load('D:\field_data\Sardon_Updated\2010\processed\ETpp30.dat') ;
21 Em = Etp30 ; % refer on ET_model eq 3.1
22 Ea = IEpositive30 ; % measured ET
23 %% 4.3 wetted evapotranspiration (priestly-Taylor)
24 Epa30_4 = (alpha) .* (esvp_30 ./ (gamma_30 + esvp_30)) .* Onpositive30 ; % refer on ET_model eq 3.1
25
26 %% 4.4 actual evapotranspiration in dimensionless
27 Ea30_Epa30_4 = ((2.*Em ./Ep30_4) ./ (1+(Em./Ep30_4)));
28
29 %% 4.5 apparent potential evapotranspiration in dimensionless
30 Epa30_Epa30_4 = 2 ./ (1 + (Em./Ep30_4));
31
32 %% 4.6 Moisture index
33 Ea30_Epa30_4 = Ea ./ Ep30_4;
34 Ea30_Epa30_4 = load('D:\field_data\Sardon_Updated\2010\processed\eaep.dat') ;
35 Ep30_Epa30_4 = load('D:\field_data\Sardon_Updated\2010\processed\ep30.dat') ;
36
37
38
39 %% 4.7 Figure
40 ET_index30_4 = figure('Position',[ 400 80 1450 800]);
41 ET_xi30_4 = axes('FontSize', 12);
42 ET_pi30_4 = plot(Ea30_Epa30_4(it),Ea30_Epa30_4(it),'.',Ea30_Epa30_4(it), Ep30_Epa30_4(it),'x');
43 xlabel('Moisture index, Ea/Ep')
44 ylabel('Normalized evaporation')
45 legend('ETa/ETp','ETp/ETp')
46 set(ET_pi30_4,'Linewidth',1,'Markersize',10)
47 saveas(ET_index30_4,'ET_index30_4.png')
48
49 %% 5. Using penman wind function
50 %% 5.1 potential evaporation
51 Ep_p5 = (esvp_d ./ (gamma_d + esvp_d)) .* Q1_d ./ lambda_d + gamma_d ./ (gamma_d + esvp_d) .* Ea5;
52
53 %% 5.2 Actual evapotranspiration
54 Ea_p5 = IE_mean_d ./ lambda_d; % ET_p ; % refer on ET_model eq 5.1
55
56 %% 5.3 wetted evapotranspiration (priestly-Taylor)

```

Appendix D Main matab M file for the Advection aridity model with three wind function



```
4 clear all
5
6 %% Pre processing
7 load010
8
9 load010postivLEON
10
11 load_filtered
12
13 load30vemarch
14
15 constants010
16
17 makedaily010
18
19 Quality
20 %% preprocessing
21 Half_hourly_products
22
23 Daily_products
24 %% Calibration
25 calibrationDaily
26 alpha
27 C_parameter_d
28 B_parameter_d
29 A_parameter_d
30 %% Processeing
31 ET_model_standard
32 ET_model_measured
33 ET_model_calibrated
34 %% Complementary relationship
35 AridityIndex_half_hourly
36
37 AridityIndex_daily
38
39 PT
40
41 PET
42
43 ET_model5
44
45 %% statistics
46
47 Erroor
48
49 liner_regression
50
```